CHAPTER 3

EXPERIMENTAL METHODS AND RESULTS

3.1 Chemicals, Apparatus and Instruments

3.1.1 Chemicals

The various chemicals used in this research project were as shown in Table 3.1.

Table 3.1 : Chemicals used in this research project.

Chemicals	Usage	Grade	Supplier
2–Hydroxyethyl methacrylate	monomer	95%	Fluka
N–Vinylpyrrolidone	monomer	97%	Fluka
Ethylene glycol dimethacrylate	crosslinking agent	> 97%	Fluka
Azo–bis–isobutyronitrile	free radical initiator	97%	BDH Chemicals
Copper(I) chloride	stabilizer	lab. reagent	Merck
Ethanol	solvent	lab. reagent	Merck
Ethanol	solvent	absolute	Merck
Methanol	solvent	lab. reagent	BDH Chemicals
Acetone	solvent	lab. reagent	Merck
Chloroform	solvent	lab. reagent	Merck
Carbon tetrachloride	solvent	lab. reagent	BDH Chemicals
Water	immersion medium	distilled	–
Sodium sulphate, anhydrous	drying agent	> 98%	Fluka
Molecular sieves Type 4 Å	drying agent	lab. reagent	Fluka
Silica gel	drying agent	lab. reagent	BDH Chemicals
Poly(ethylene terephthalate) film	mould release agent	commercial	3M

3.1.2 Apparatus and Instruments

The major items of equipment used in this project were as shown in Table 3.2.

Table 3.2 : Apparatus and instruments used in this work.

Apparatus and Instruments	Company	Model
Vacuum Oven	Eyela	VOS–300SD
Incubator	Memmert	–
Drying Oven	Thelco	–
Infrared Spectrometer	Jasco	810
FT–IR Spectrometer	Nicolet	510
Elemental Analyzer (CHNS/O)	Perkin–Elmer	PE–2400 Series II
Thermogravimetric Analyzer	Perkin–Elmer	TGA 7
KBr Press	Jasco	–
Universal Testing Machine	Shimadzu	Autograph AGS–500 A
Tensile Specimen Press	Kao Tieh	KT–7016

3.2 Purification and Analysis of Initiator, Monomers and Crosslinking Agent

3.2.1 Recrystallization of Initiator

The azo–bis–isobutyronitrile, AIBN, free radical initiator used in this work needed to be purified by recrystallization before it could be used in polymerization. This recrystallization was carried out, as shown in Fig. 3.1, by first dissolving about 1.5 g of AIBN in 150 ml of an absolute ethanol : water (1:1 v/v) solvent mixture at about 70°C. The solution was then filtered through a filter paper (Whatman No.1) and the AIBN allowed to recrystallize in a refrigerator at 0–5°C. The crystals obtained were filtered through a sintered glass filter (porosity 4) and were then dried

to constant weight in a vacuum oven at 40°C to remove any remaining traces of solvent. The yield was typically about 70%. Finally, the crystals were stored in the dark in a refrigerator until required for use.

The IR spectrum of the recrystallized product is shown in Fig. 3.2 and can be compared with the reference spectrum in Fig. 3.3. The main vibrational band assignments are given in Table 3.3.

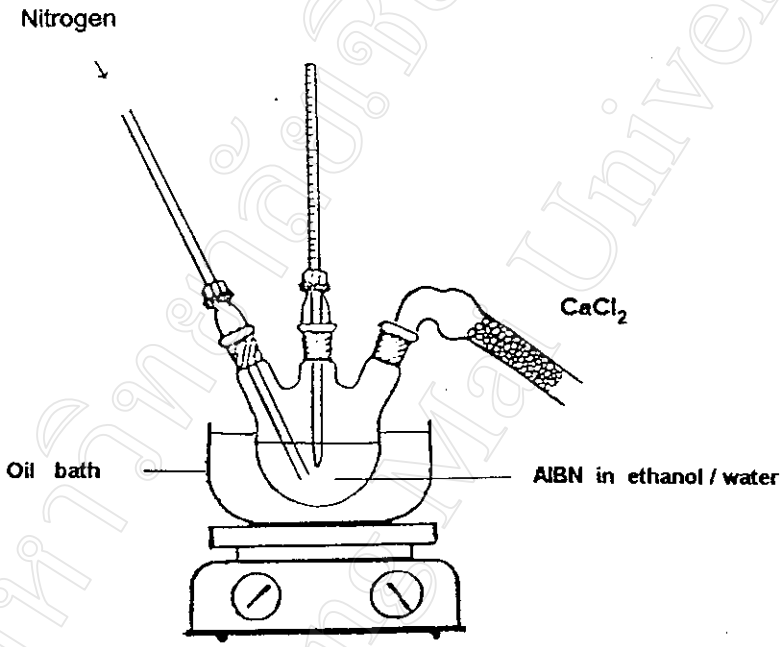

Fig. 3.1 : Apparatus used for purification of azo–bis–isobutyronitrile : dissolution prior to recrystallization.

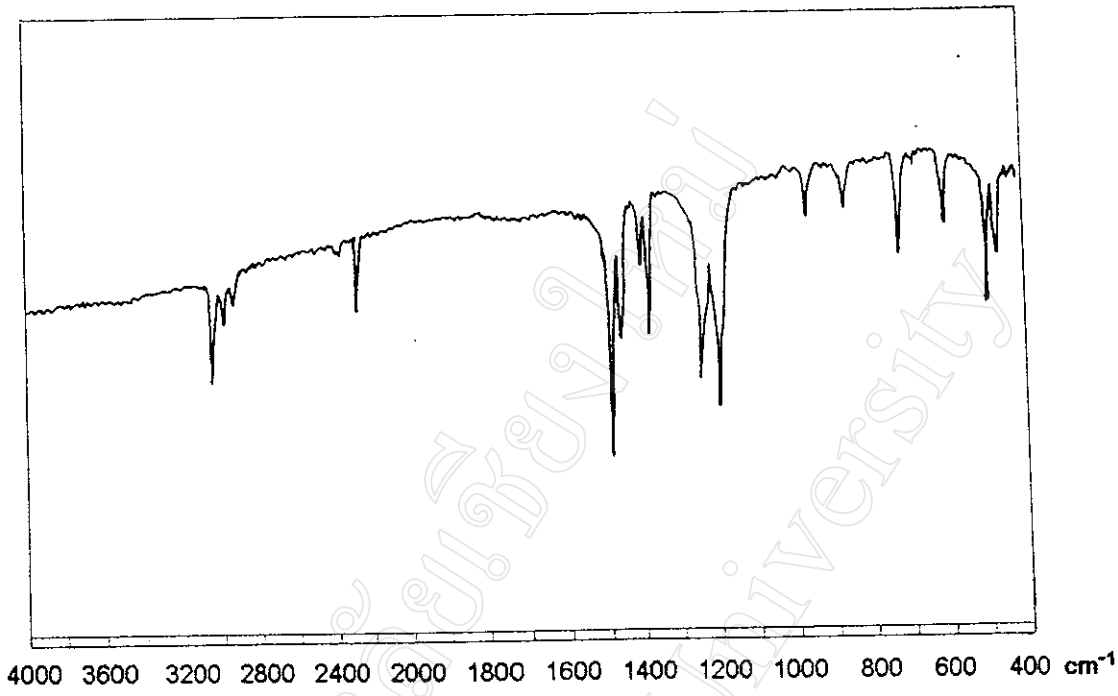

Fig. 3.2 : Infrared spectrum of recrystallized azo–bis–isobutyronitrile.

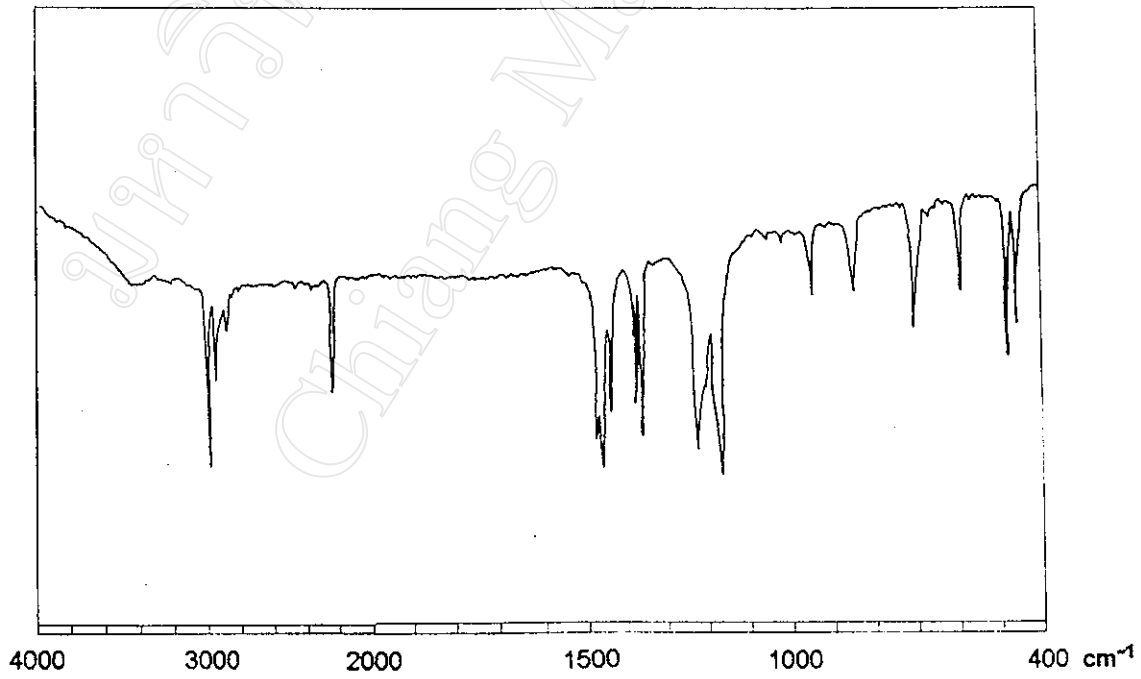

Fig. 3.3 : Reference infrared spectrum of azo–bis–isobutyronitrile [33].

Table 3.3 : Infrared absorption band assignments for purified azo–bis–isobutyronitrile.

Vibrational Assignments	Wavenumber (cm^{-1})
C–H stretching	3100–2950
C–H bending	1500, 1380
N=N stretching	see NOTE below
C–N stretching	1230
C≡N stretching	2260

NOTE : The N=N stretching vibration of a symmetrical trans azo compound is forbidden in the infrared but absorbs in the 1576 cm^{-1} region of the Raman spectrum [34].

The chemical structure of azo–bis–isobutyronitrile is as shown below :

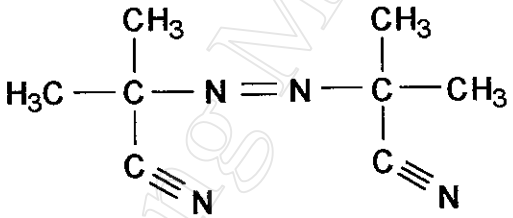

The AIBN sample for IR analysis was prepared in the form of a KBr disc and the spectrum run on a Jasco IR–810 Infrared Spectrometer .

On comparing the AIBN sample and reference spectra in Figs. 3.2 and 3.3, they are seen to be almost identical in appearance. This high degree of similarity can be taken as an indicator of the high degree of purity of the recrystallized product.

3.2.2 Vacuum Distillation of Monomers

The main reason for using vacuum distillation for the purification of the monomers used in this project was that both the 2–hydroxyethyl methacrylate and N–vinylpyrrolidone can thermally self–polymerize at their normal boiling points at atmospheric pressure. The vacuum distillation apparatus used was as shown in Fig. 3.4.

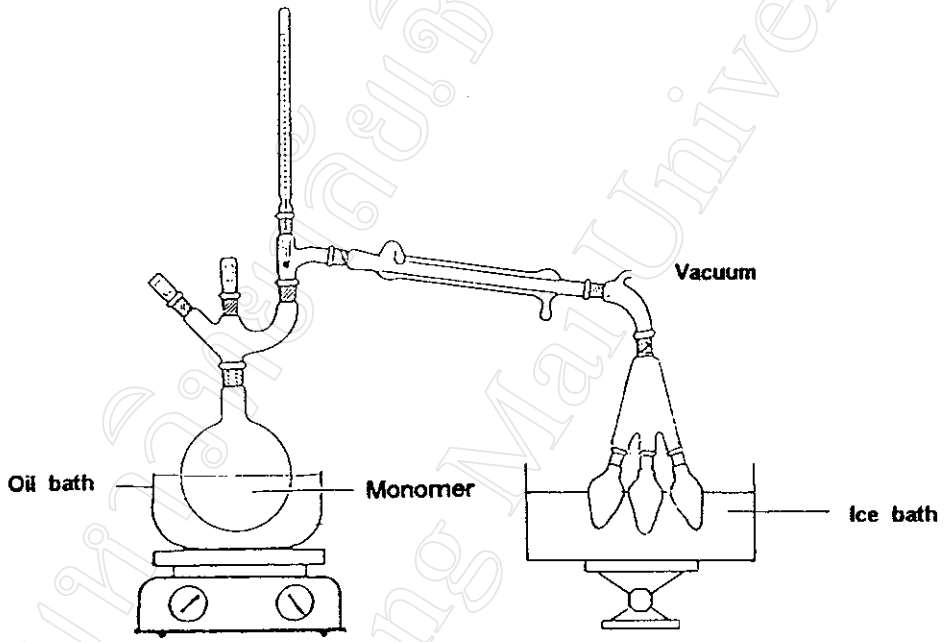

Fig. 3.4 : Vacuum distillation apparatus used in the purification of monomers.

3.2.2.1 2–Hydroxyethyl Methacrylate

The 2–hydroxyethyl methacrylate monomer (Fluka, assay ≈ 95%), as supplied, was first dried with anhydrous sodium sulphate. After occasional tumbling, the monomer was left to stand over the drying agent for at least one hour before vacuum distillation.

In the vacuum distillation that followed, a multi–limb receiver adapter was used which allowed more than one fraction to be collected without disturbing the system. After decanting the 2–hydroxyethyl methacrylate monomer away from the drying agent, about 1 g/l of copper(I) chloride was added to the monomer as stabilizer and the monomer distilled under vacuum. Pure 2–hydroxyethyl methacrylate was collected as the constant boiling fraction at 68°C / 2–3 mm Hg pressure (cf. lit. [35] b.p. 67°C / 3–5 mm Hg). The initial 10% volume fraction of distillate was discarded. The distilled 2–hydroxyethyl methacrylate was then stored in the refrigerator (freezer compartment) until required for use in polymerization.

The IR spectrum of the distilled monomer is shown in Fig. 3.5 and can be compared with the reference spectrum in Fig. 3.6. The major vibrational peaks present are listed in Table 3.4 below. The monomer spectrum was obtained from a neat sample contained in a NaCl cell.

Table 3.4 : Infrared absorption band assignments for distilled 2–hydroxyethyl methacrylate.

Vibrational Assignments	Wavenumber (cm^{-1})
O–H stretching	3700–3300
C–H stretching	3000–2800
C=O stretching	1730
C=C stretching	1650
C–H bending, in CH_2	1480, 1420
C–H bending, in CH_3	1380
C–O stretching, acyl–oxygen	1300
C–O stretching, alkyl–oxygen	1150

The chemical structure of 2–hydroxyethyl methacrylate is as shown below :

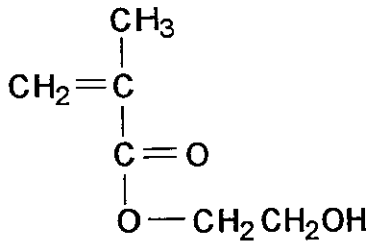

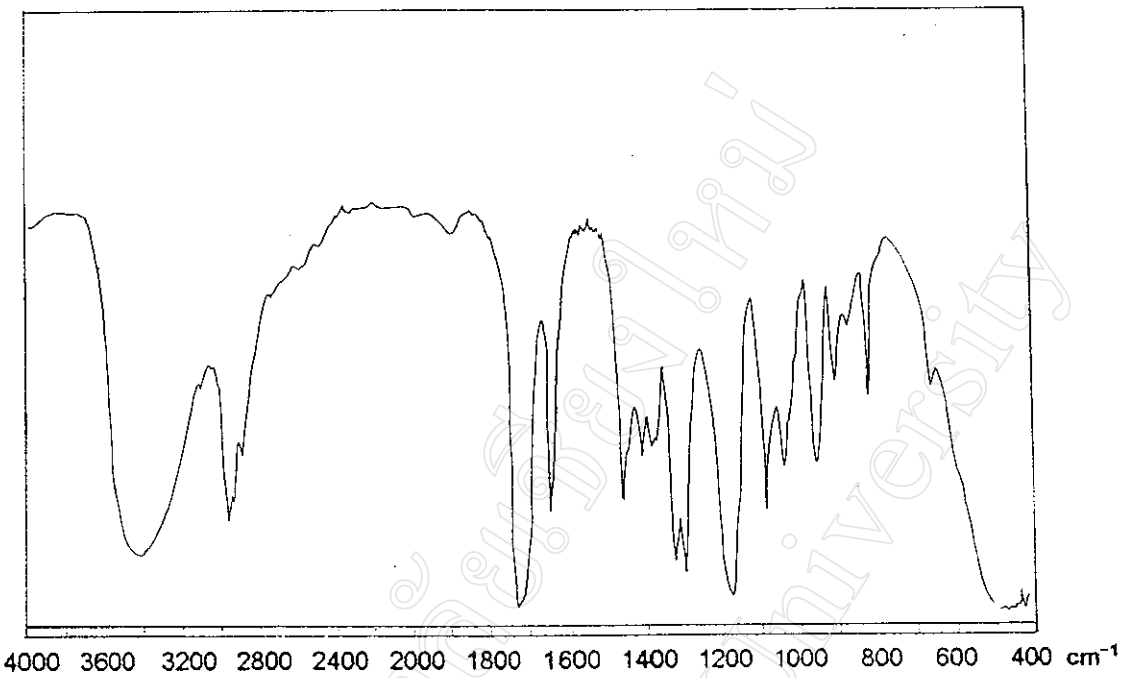

Fig. 3.5 : Infrared spectrum of distilled 2–hydroxyethyl methacrylate.

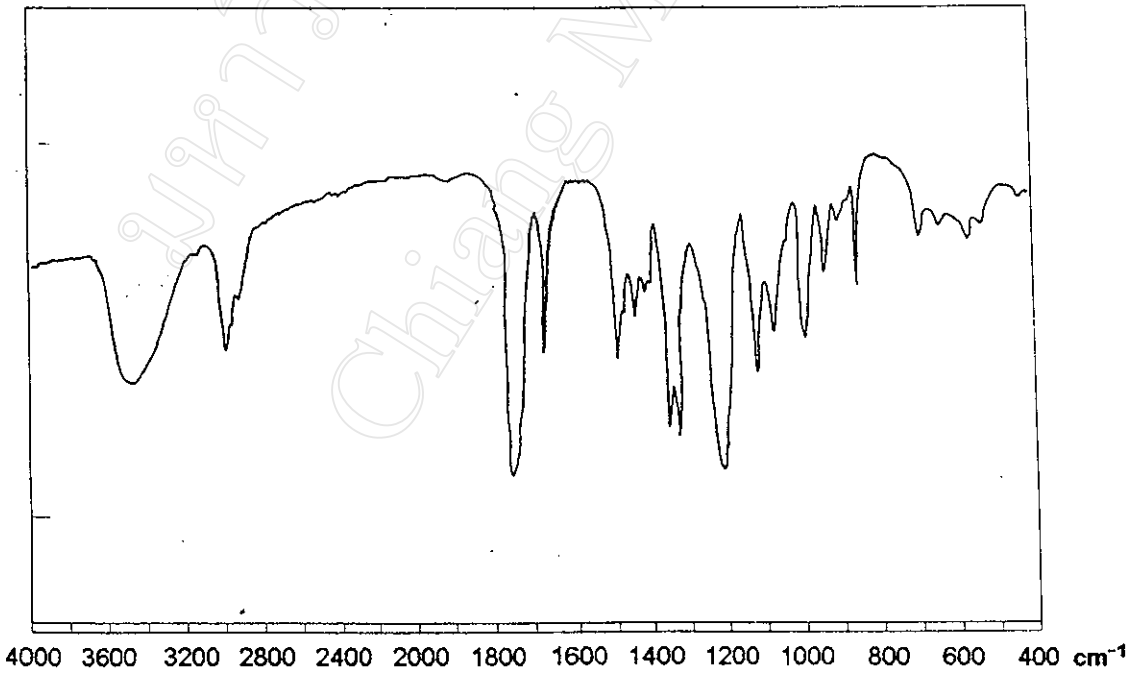

Fig. 3.6 : Reference infrared spectrum of 2–hydroxyethyl methacrylate [36].

3.2.2.2 N–Vinylpyrrolidone

The N–vinylpyrrolidone monomer (Fluka, assay ≈ 97%) was also purified by vacuum distillation. The procedure used was similar to that for 2–hydroxyethyl methacrylate, as described in the previous section 3.2.2.1. The constant boiling fraction at 65°C / 2–3 mm Hg pressure was collected (cf. lit. [37] b.p. 87°C / 5–8.5 mm Hg).

The IR spectrum of the distilled N–vinylpyrrolidone monomer is shown in Fig. 3.7 and can be compared with the reference spectrum in Fig. 3.8. The major vibrational peaks are listed in Table 3.5 below and are seen to be consistent with and confirmative of the chemical structure of N–vinylpyrrolidone.

Table 3.5 : Infrared absorption band assignments for distilled N–vinylpyrrolidone.

Vibrational Assignments	Wavenumber (cm^{-1})
C–H stretching	2950
C=O stretching	1730
C=C stretching	1650
C–H bending	1480
C–N stretching	1250

The chemical structure of N–vinylpyrrolidone is as shown below :

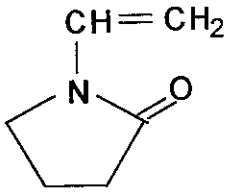

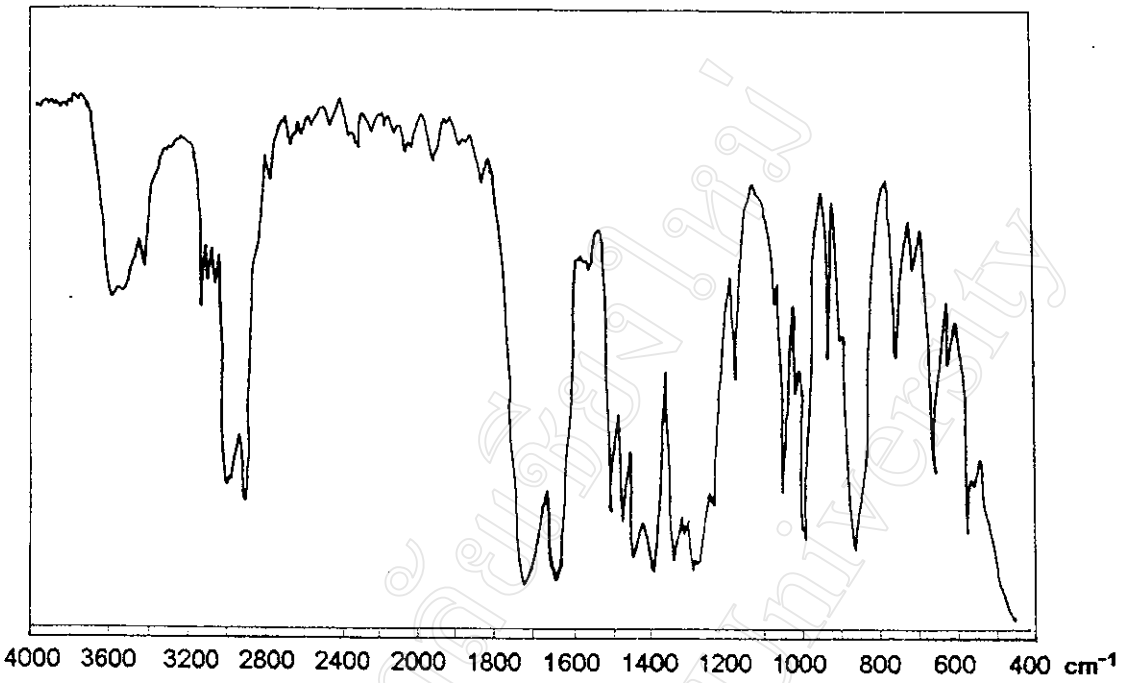

Fig. 3.7 : Infrared spectrum of distilled N–vinylpyrrolidone.

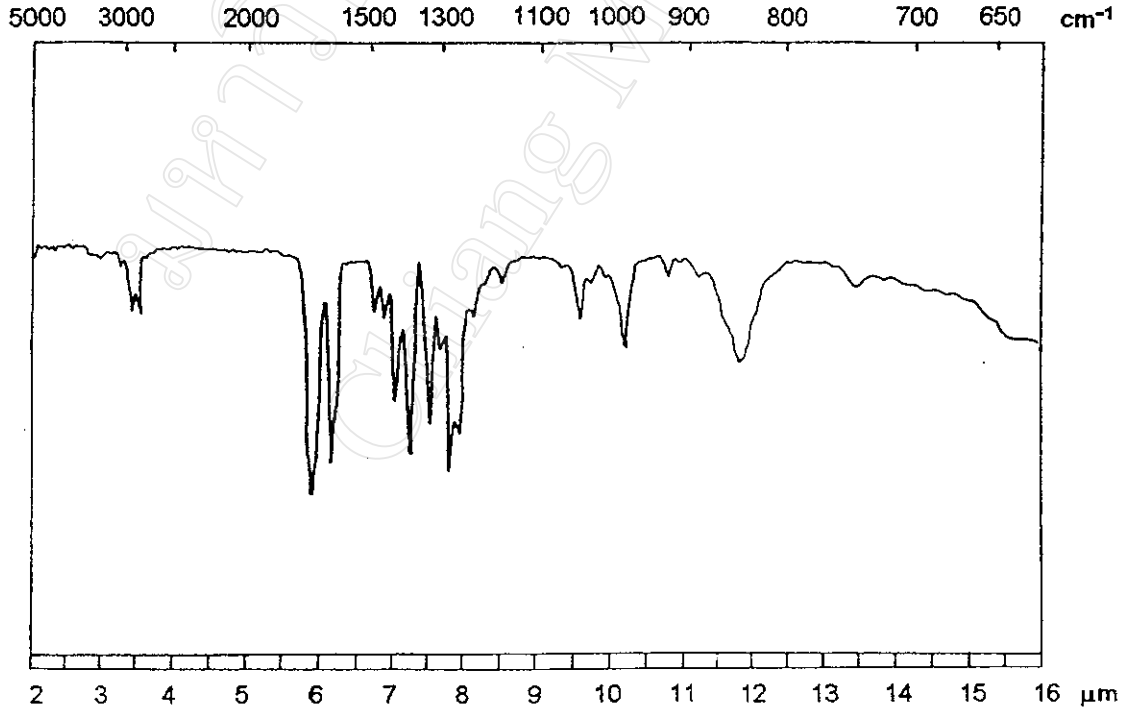

Fig. 3.8 : Reference infrared spectrum of N–vinylpyrrolidone [38].

3.2.3 Vacuum Distillation of Crosslinking Agent

The ethylene glycol dimethacrylate crosslinking agent was also purified by vacuum distillation using the same apparatus as for the monomers previously (Fig. 3.4). Firstly, the ethylene glycol dimethacrylate was pre–dried with anhydrous sodium sulphate to absorb moisture. In the vacuum distillation that followed, pure ethylene glycol dimethacrylate was collected as the constant boiling fraction at 98°C / 2–3 mm Hg pressure (cf. lit. [35] b.p. 98–100°C / 5 mm Hg). It was then stored in the refrigerator (freezer compartment) until required for use.

The distilled ethylene glycol dimethacrylate IR spectrum shown in Fig. 3.9 can be compared with the reference spectrum in Fig. 3.10. The major vibrational peaks are assigned shown in Table 3.6 below in relation to the chemical structure which is also shown.

Table 3.6 : Infrared absorption band assignments for distilled ethylene glycol dimethacrylate.

Vibrational Assignments	Wavenumber (cm^{-1})
C–H stretching	2950
C=O stretching	1750
C=C stretching	1650
C–H bending	1480, 1420
C–O stretching, acyl–oxygen	1300
C–O stretching, alkyl–oxygen	1150

The chemical structure of ethylene glycol dimethacrylate is as shown below :

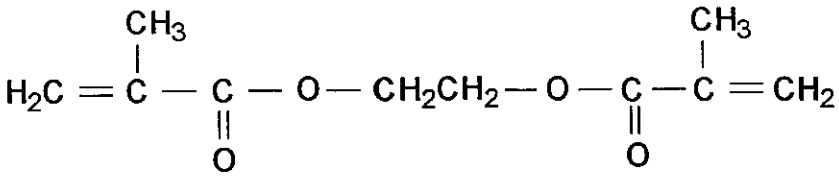

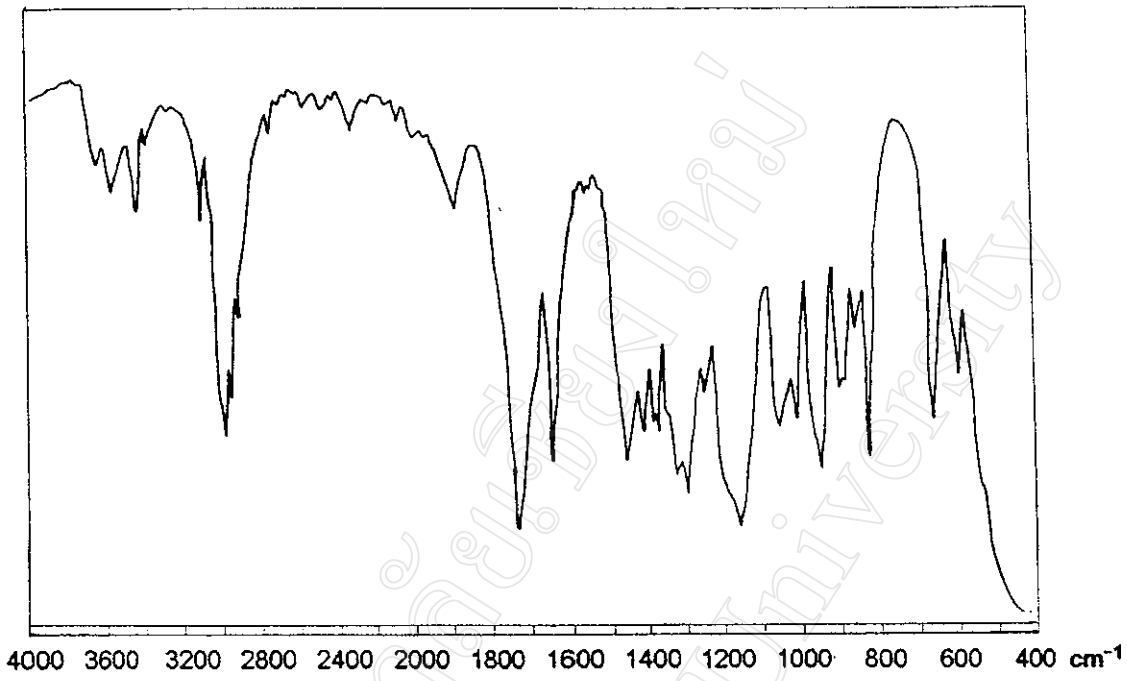

Fig. 3.9 : Infrared spectrum of distilled ethylene glycol dimethacrylate.

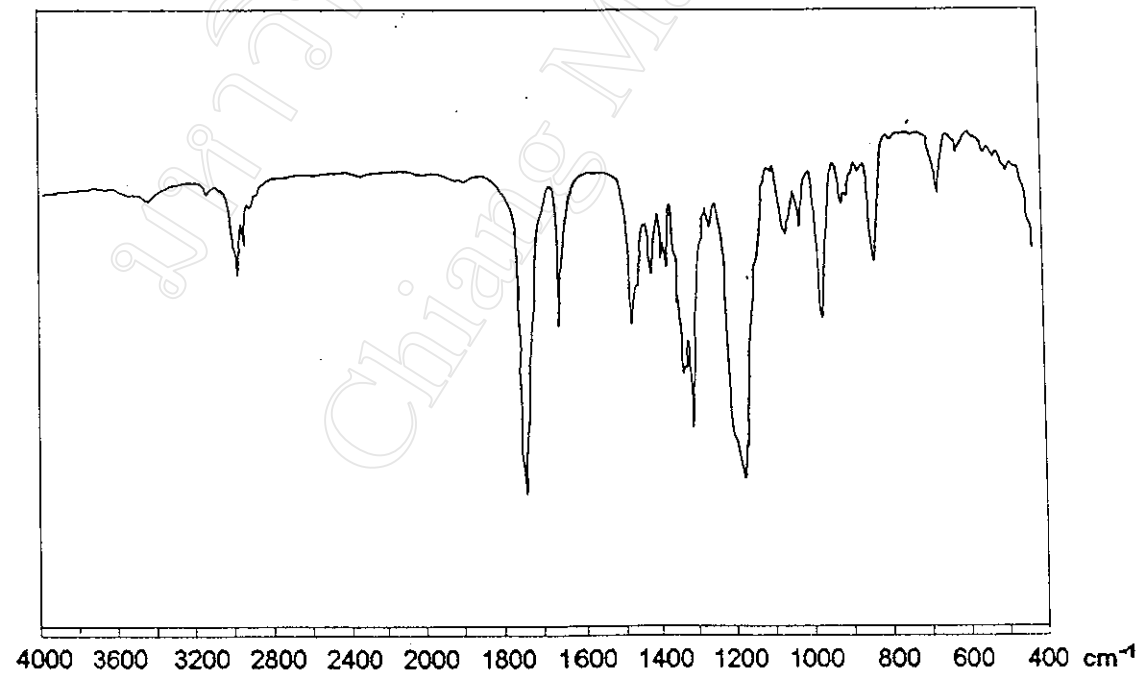

Fig. 3.10 : Reference infrared spectrum of ethylene glycol dimethacrylate [36].

3.3 Bulk Polymerization in the Form of Thin Sheets

3.3.1 Mould Design

The mould consisted of two Perspex (poly(methyl methacrylate)) plates (10 cm × 12 cm × 0.8 cm), each lined on the inside with thin PET (polyethylene terephthalate) films to permit ease of separation and sample removal. A thin wire covered with Teflon (polytetrafluoroethylene) tape, which functioned as a gasket (0.5 mm thickness) in between the PET films, created the internal void space into which the polymerization mixture was injected. The two Perspex plates were held tightly together by means of four screws and nuts. A diagram of the mould is shown below in Fig. 3.11.

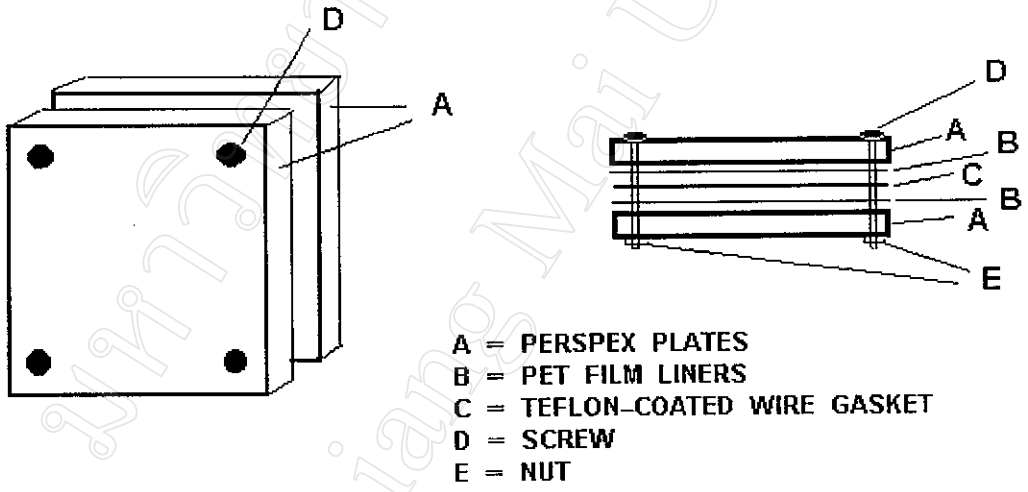

Fig. 3.11 : Mould used for bulk polymerization in the form of thin sheets.

3.3.2 Bulk Polymerization / Copolymerization Procedure

Thin sheets of polymer were produced by *'in situ'* bulk polymerization of the monomer mixture in the mould as described above in section 3.3.1. The monomers were mixed together with the azo–bis–isobutyronitrile (0.5 % w/w) initiator and

ethylene glycol dimethacrylate crosslinking agent (1.0 % w/w) at low temperature (0 – 5°C) until a homogeneous clear solution was obtained. In this research project, 2–hydroxyethyl methacrylate (HEMA) and N–vinylpyrrolidone (VP) were the monomers used in polymerization. The various comonomer feed compositions used are shown in Table 3.7. Each mixture was outgassed with nitrogen before injection into the mould. The mould was then placed in an oven at 60°C for 3 days followed by 2 hours postcure at 90°C under vacuum in order to remove any residual monomer. The thin sheets of polymer obtained were of 0.5 ± 0.1 mm thickness, as determined by a micrometer at ten different places.

Table 3.7 : Comonomer feed compositions used in copolymer synthesis.

Polymers	Comonomer Feed Compositions	
	HEMA (wt.%)	VP (wt.%)
P(HEMA)	100	0
P(HEMA–co–VP)	95	5
P(HEMA–co–VP)	90	10
P(HEMA–co–VP)	85	15
P(HEMA–co–VP)	80	20
PVP	0	100

The rationale used in the choice of comonomer feed compositions was that the HEMA monomer is intended to be the major component in the resultant copolymer. The VP comonomer is the minor component intended to modify the properties of P(HEMA), as will be described in the following sections.

3.4 Polymer Characterization

3.4.1 Polymer Properties Relevant to Intended Application

Some properties of the thin sheet products obtained which are relevant to their intended use as temporary skin substitutes are shown in Table 3.8.

Table 3.8 : Some properties of the dry and hydrated polymer sheets relevant to wound coverings.

Polymer Properties	Dry Polymers		Hydrated Polymers *	
	P(HEMA)	P(HEMA-co-VP)	P(HEMA)	P(HEMA-co-VP)
Transparency	transparent	transparent	transparent	transparent
Colour	colourless	slightly yellowish	colourless	slightly yellowish
Adhesion to skin surface	non–adhesive	non–adhesive	slightly adhesive	slightly more than P(HEMA)
Flexibility	fairly stiff	fairly stiff	flexible	more flexible than P(HEMA)

* the polymer was hydrated in distilled water to equilibrium at room temperature for at least 1 day

3.4.2 Solubility [39]

Crosslinked polymers, such as those synthesized in this work, do not show normal solubility. Although such polymers may swell under the influence of certain solvents, swelling in itself is not proof of crosslinking, since a polymer on the borderline of solubility may also exhibit this behavior. However, when a polymer resists solubility in a number of solvents typical for those of its class, and is infusible as well, it is usually considered to be crosslinked unless there is compelling evidence to the contrary.

Many of the structural aspects of polymer molecules that affect solubility and the melting point are those that affect these same properties in simple organic molecules. For instance, crystallinity, high symmetry, hydrogen bonding, high polarity, chain stiffness and stereoregularity in the chain, contribute to a higher melting point and reduced solubility compared to an otherwise similar polymer lacking the feature in question. The following procedure, as employed here, is useful for the rapid determination of polymer solubility.

A small piece of the polymer was mixed with about 5 ml of solvent in a test tube and stirred together thoroughly. (Solubility is usually facilitated by the use of polymer in a finely divided state.) If no sign of solubility occurred at room temperature, the mixture was heated gently at or just below the boiling point of the solvent. If the polymer dissolved, the solution was allowed to cool to see if the polymer remained in solution or precipitated. If the polymer was swollen by the solvent but was not dissolved, other related solvents were checked to see if they could effect solution, either singly or in combination.

The solubility test results for **uncrosslinked** P(HEMA) are shown in Table 3.9 below.

Table 3.9 : Solubility test results for uncrosslinked P(HEMA).

Solvent	Solubility test	
	Cool solvent	Hot solvent
Ethanol	×	×
Methanol	×	×
Acetone	×	×
Chloroform	×	×
Carbon tetrachloride	×	×
Benzene : Ethanol = 1:1	×	✓
Water	×	×

Notation : × = insoluble

✓ = soluble at about 70°C

3.4.3 Infrared Spectroscopy

Infrared spectroscopic techniques are widely used in polymer investigations in a variety of applications. In addition to their qualitative analysis for structural characterization, infrared spectra may also be analyzed quantitatively for following microstructural changes (e.g., differences in copolymer composition) by determination of the absorbance ratio of functional groups through their characteristic absorption frequencies. In this research project, a Nicolet FT–IR 510 Infrared Spectrometer was used to characterize and compare the chemical structures of the P(HEMA) homopolymer and P(HEMA–co–VP) copolymers.

The infrared spectra of both the uncrosslinked and crosslinked P(HEMA) samples are shown in Figs. 3.13 and 3.14. The crosslinked P(HEMA–co–VP) copolymers obtained from the different monomer feed compositions are featured in Figs. 3.15 – 3.18. A brief structural interpretation of these spectra is detailed in Table 3.10. The spectra were obtained with the samples in the form of KBr discs since the polymers could not be dissolved in common organic solvents.

Fig. 3.12 : The Nicolet Model FT–IR 510 Infrared Spectrometer.

Table 3.10 : Structural interpretation of the infrared spectra (Figs. 3.13 – 3.18) of the P(HEMA) homopolymers and P(HEMA–co–VP) copolymers from different comonomer feed compositions.

Vibrational Assignments	Unit *	Wavenumber (cm^{-1})
O–H stretching	HEMA	3700–3300
C–H stretching, aliphatic	both	3000–2800
C=O stretching	HEMA	1730
C=O stretching	VP	1650
C–H stretching, alicyclic	VP	1480, 1420
C–H bending	both	1380
C–O stretching, acyl–oxygen	HEMA	1300
C–N stretching	VP	1250
C–O stretching, alkyl–oxygen	HEMA	1150

* the respective chemical structures of the HEMA and VP repeat units in the copolymer chain are as shown below :

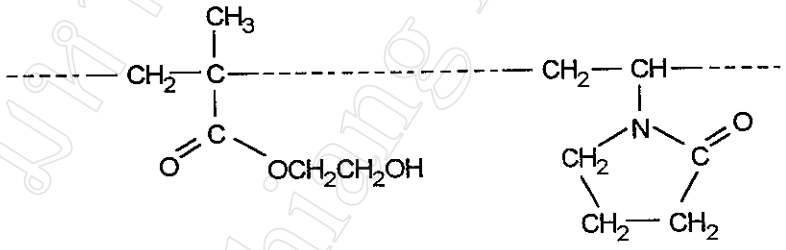

HEMA unit **VP unit**

On comparing the IR spectra, the most notable feature is the increase in intensity of the second carbonyl (C=O) stretching peak at around 1650 cm^{-1} as the amount of VP monomer in the initial comonomer feed increases. Apart from this feature, the copolymer spectra are dominated by the peaks derived from the HEMA units as the major component.

sample uncrosslinked P(HEMA)
sample date
Thu, Apr 27, 1995, 15:29:12

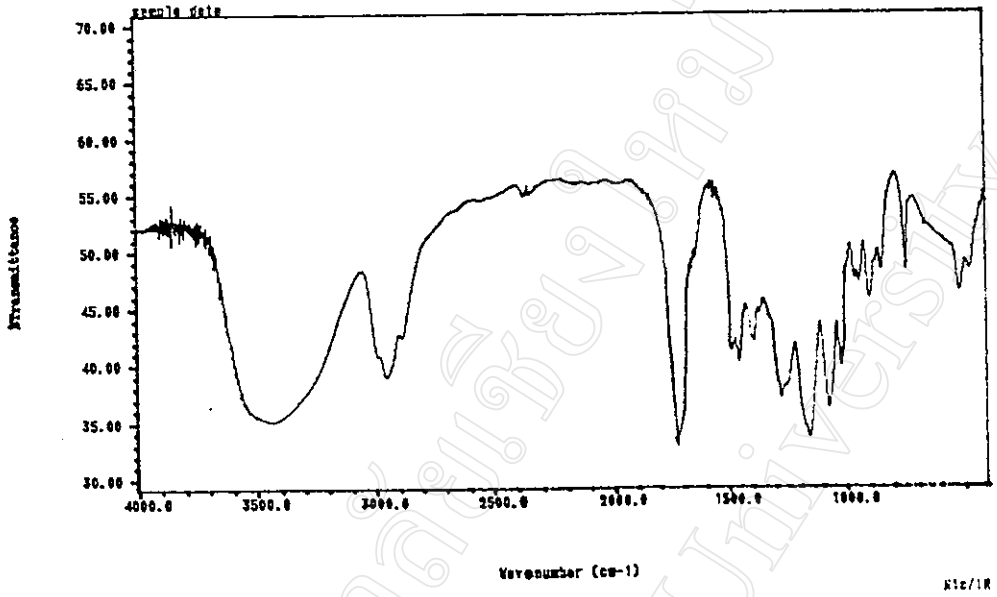

Fig. 3.13 : Infrared spectrum of uncrosslinked P(HEMA).

sample crosslinked P(HEMA)
sample date
Thu, Apr 27, 1995, 16:06:16

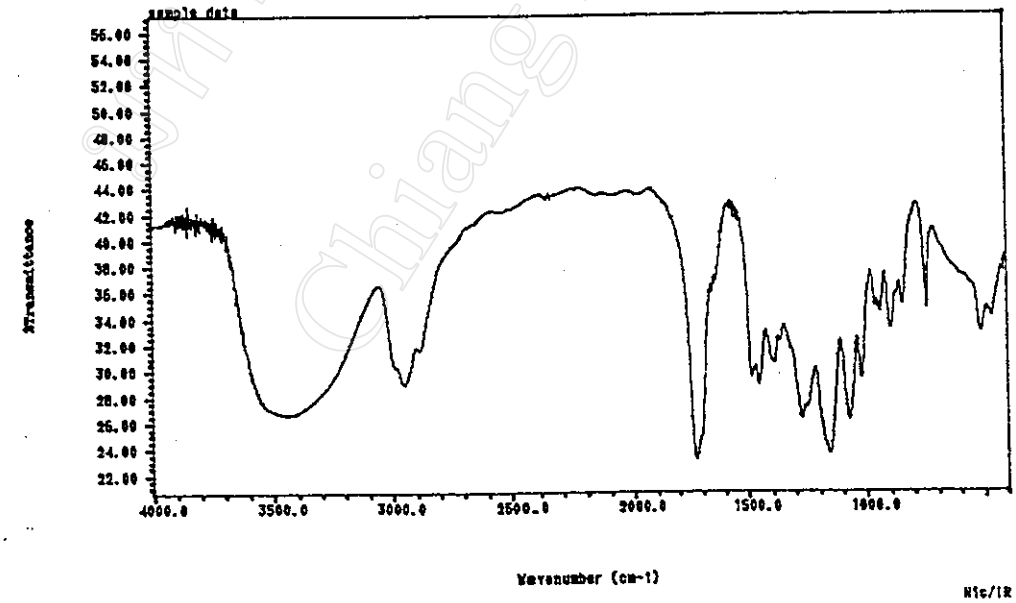

Fig. 3.14 : Infrared spectrum of crosslinked P(HEMA).

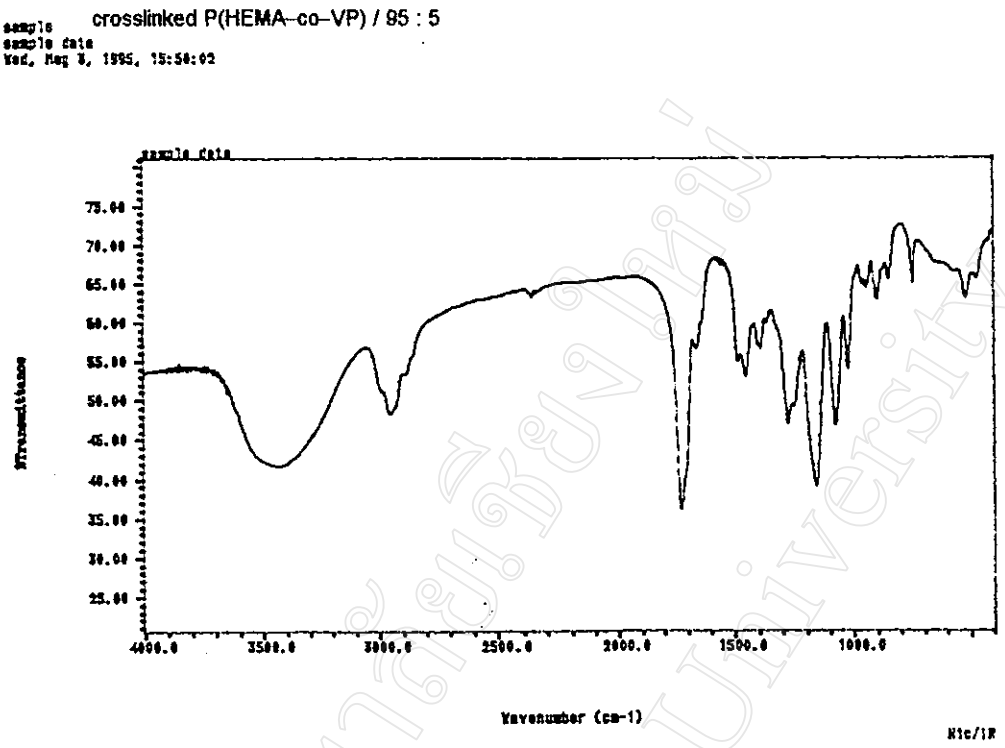

Fig. 3.15 : Infrared spectrum of crosslinked P(HEMA–co–VP) / 95 : 5.

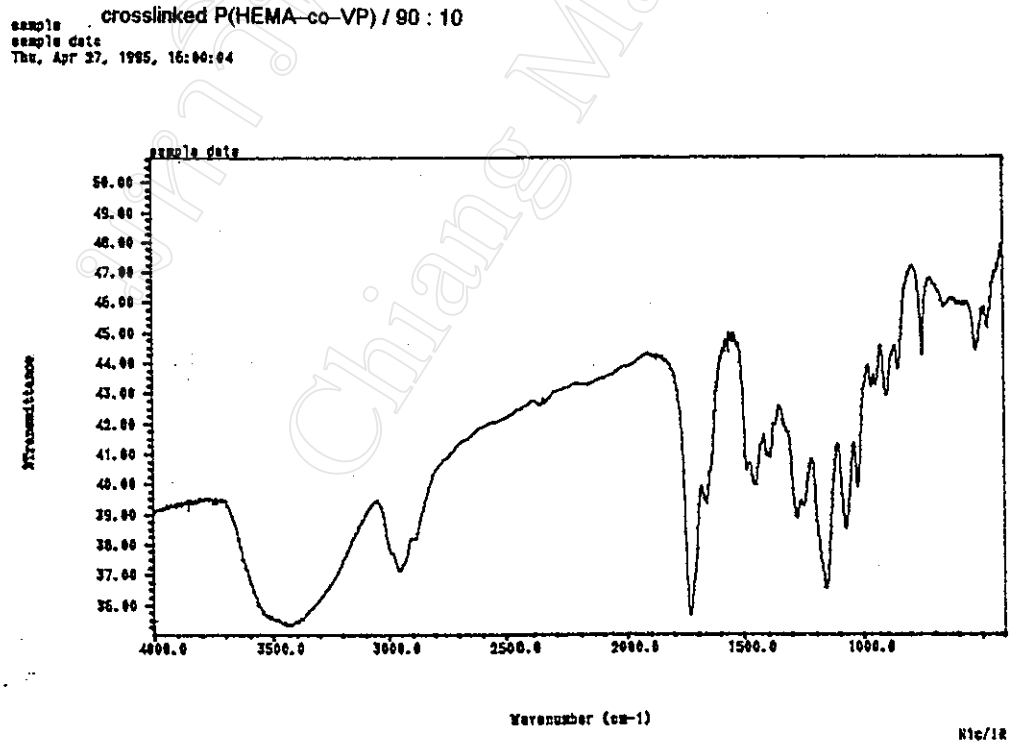

Fig. 3.16 : Infrared spectrum of crosslinked P(HEMA–co–VP) / 90 : 10.

sample crosslinked P(HEMA–co–VP) / 85 : 15
sample date
Thu, Apr 27, 1995, 16:13:02

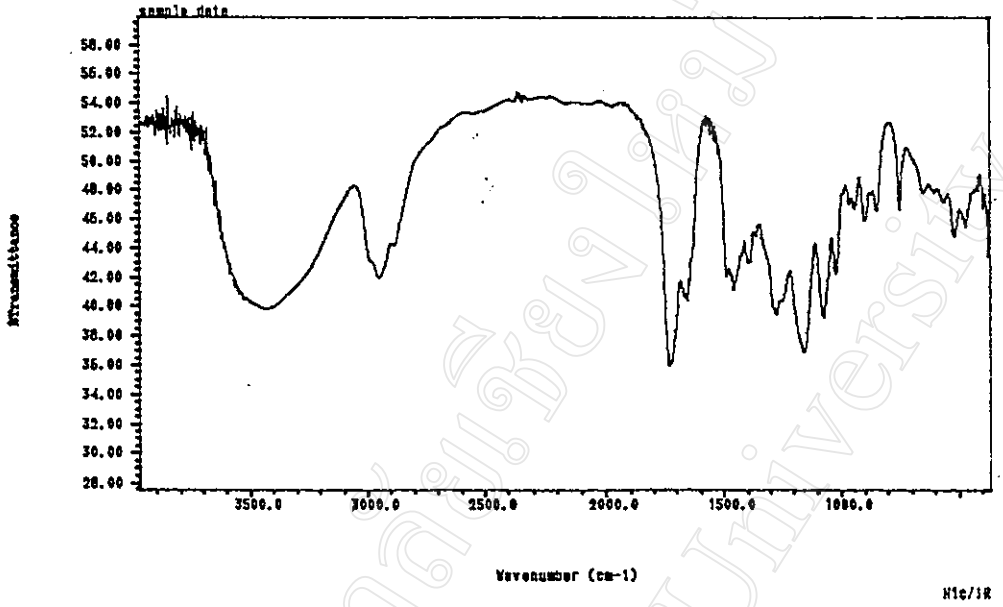

Fig. 3.17 : Infrared spectrum of crosslinked P(HEMA–co–VP) / 85 : 15.

sample crosslinked P(HEMA–co–VP) / 80 : 20
sample date
Thu, Apr 27, 1995, 16:19:55

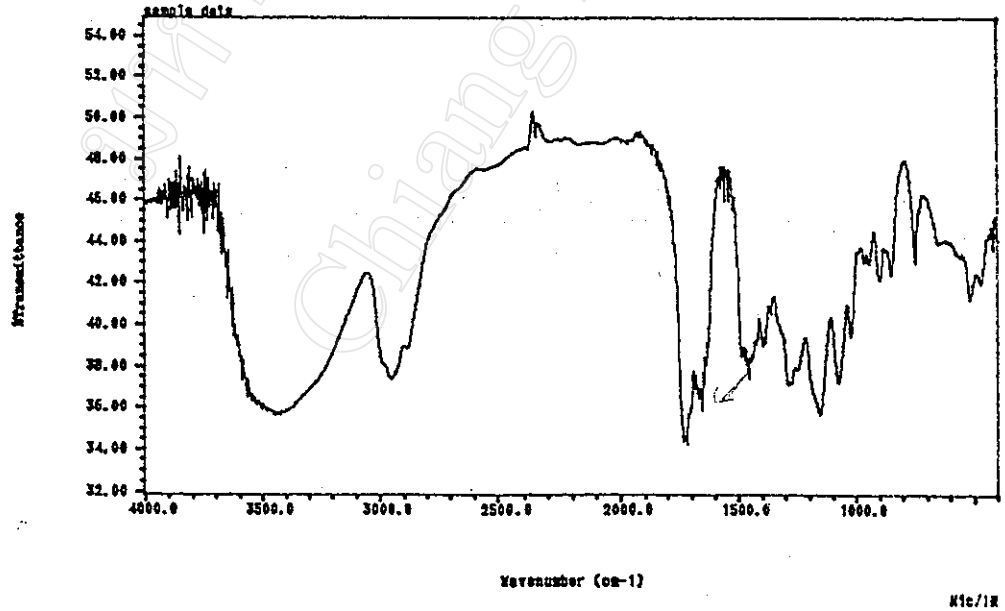

Fig. 3.18 : Infrared spectrum of crosslinked P(HEMA–co–VP) / 80 : 20.

3.4.4 Elemental Analysis [40]

Elemental analysis is particularly useful in copolymer characterization. Since copolymers are usually composed of the elements carbon, hydrogen, nitrogen, sulphur and oxygen, the percentages of which can be determined by elemental (CHNS/O) analysis, the corresponding percentages of each monomer in the copolymer can be calculated.

A Perkin–Elmer PE 2400 Series II CHNS/O Analyzer was used in this study for the rapid determination of the carbon, hydrogen, nitrogen and oxygen contents in the copolymers. The PE 2400 Series II Analyzer is capable of operating in multiple analysis modes. These modes include the simultaneous determination of carbon, hydrogen and nitrogen (option 1, CHN), carbon, hydrogen, nitrogen and sulphur (option 2, CHNS), and the determination of oxygen (option 3, oxygen). Fig. 3.19 shows the PE 2400 Series II CHNS/O Analyzer, Data Printer and Perkin–Elmer AD–6 Ultramicrobalance. The operational specifications for the CHNS/O options used in this research project were :

SAMPLE TYPE	:	solids and liquids
TIME	:	8 minutes
ACCURACY	:	plus/minus 0.3%
SAMPLE SIZE	:	1–2 mg

Fig.3.19 : The Perkin–Elmer PE 2400 Series II CHNS/O Analyzer (centre) showing also the Data Printer (left) and the Perkin–Elmer AD–6 Ultramicrobalance (right).

In its CHN operating mode (option 1), the PE 2400 Series II CHNS/O Analyzer uses a combustion method to convert the sample elements to simple gases. The sample is first oxidized in a pure oxygen environment using classical reagents. Products produced in the combustion zone include CO_2, H_2O and N_2. Other elements, such as halogens and sulphur, are removed by scrubbing reagents in the combustion zone. The resulting gases are homogenized and controlled to exact conditions of pressure, temperature and volume. The homogenized gases are allowed to de–pressurize through a column where they are separated in a stepwise steady–state manner and detected as a function of their thermal conductivity.

In its oxygen operating mode (option 3), the PE 2400 Series II CHNS/O Analyzer performs oxygen analysis. The sample is pyrolyzed in a helium / hydrogen environment at 1000°C over platinized carbon, whereupon the pyrolyzed oxygen products of reaction are converted to carbon monoxide. The carbon monoxide and other gases pass through a scrubber trap where acid gases and water are removed. In a similar manner to option 1, the resulting gases are then homogenized and controlled to exact conditions of pressure, temperature and volume. The homogenized gases are again allowed to de–pressurize through a column where they are separated in a stepwise steady–state manner and detected as a function of their thermal conductivity. A helium / hydrogen (or argon / hydrogen) carrier gas mixture is used in this procedure to enhance the conversion of oxygen to carbon monoxide.

A summary of the results obtained from elemental analysis of the polymers synthesized in this project is given in Table 3.11. In the case of the two homopolymers, P(HEMA) and PVP, their elemental compositions are already known and so their calculated % compositions from the CHNO data can be compared with the corresponding theoretical values. However, in the case of the P(HEMA–co–VP) copolymers, their exact compositions are unknown. The results in Table 3.11 therefore provide a means of determining the copolymer compositions. This is most conveniently done by comparing their nitrogen contents (from the VP units) with the calibration curve in Fig. 3.20.

Table 3.11 : Elemental analysis results including copolymer compositions.

Homopolymers	Carbon (wt.)		Hydrogen (wt.)		Nitrogen (wt.)		Oxygen (wt.)	
	Theoretical	Found	Theoretical	Found	Theoretical	Found	Theoretical	Found
uncrosslinked P(HEMA)	**55.36**	52.30	**7.76**	8.04	–	0.38	**36.88**	38.70
crosslinked P(HEMA)	**55.36**	52.64	**7.76**	8.14	–	0.40	**36.88**	38.46
uncrosslinked PVP	**64.83**	61.86	**8.18**	8.61	**12.60**	12.03	**14.39**	18.02
crosslinked PVP	**64.83**	61.74	**8.18**	9.00	**12.60**	11.68	**14.39**	18.47

Copolymers	Carbon Wt.% Found	Hydrogen Wt.% Found	Nitrogen Wt.% Found	Oxygen Wt.% Found	Composition (wt.%) HEMA : VP
P(HEMA-co-VP) / 95:5	53.06	8.16	1.01	37.96	92 : 8
P(HEMA-co-VP) / 90:10	53.26	8.36	1.44	37.38	88 : 12
P(HEMA-co-VP) / 85:15	54.01	8.15	2.02	36.29	84 : 16
P(HEMA-co-VP) / 80:20	54.25	8.38	2.53	37.01	81 :19

NOTES : (1) The calculated theoretical values do not take into account the small amount (1% by wt.) of crosslinking agent used.

(2) The copolymer compositions were calculated from the % N contents with reference to Fig. 3.20.

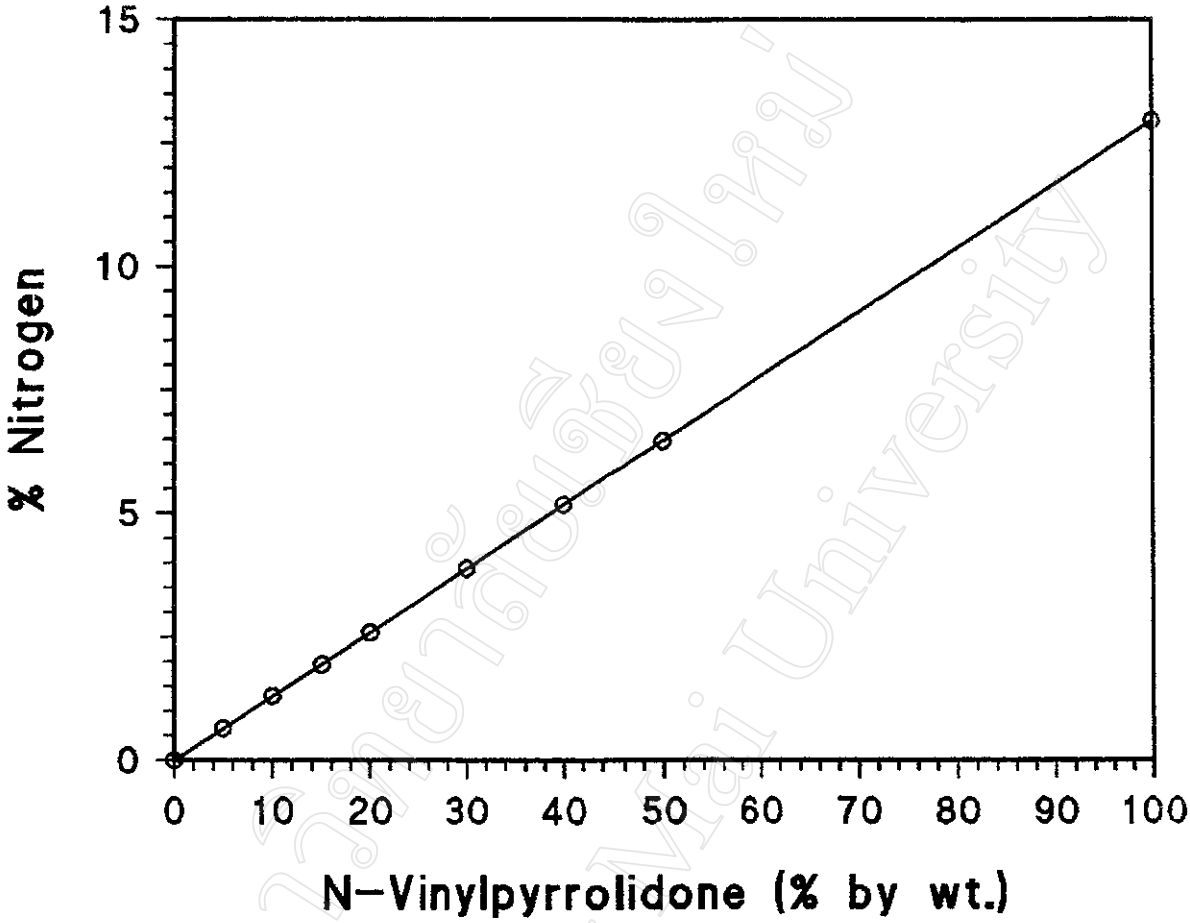

Fig. 3.20 : Theoretical calibration curve of % N content (by weight) against % vinylpyrrolidone (by weight) in P(HEMA–co–VP) copolymers.

3.4.5 Thermogravimetry [38]

Thermogravimetry (TG) is defined by the ICTAC (International Confederation for Thermal Analysis and Calorimetry) [39] as : **"A technique in which the mass of a substance is measured as a function of temperature while the substance is subjected to a controlled temperature program"**

There are 3 modes of thermogravimetry : in **Isothermal Thermogravimetry**, the sample mass is recorded as a function of time at constant temperature. In **Quasi–Isothermal Thermogravimetry**, the sample is heated to constant mass at each of a series of increasing temperatures. This technique is often titled **Controlled–Rate Thermogravimetry**. Finally, in **Dynamic Thermogravimetry**, the sample is heated in an environment, the temperature of which varies at a predetermined constant rate.

Thermogravimetry is a very versatile analytical technique and thus its application range is diverse and extensive. TG has been used extensively to quantitatively determine the components of a mixture. A wide variety of organic, inorganic, organometallic and coordination compounds, including polymers, have been studied by TG in order to determine their associated thermal stabilities and thermal decomposition characteristics. TG has also been extensively used for "fingerprinting" and assaying organic compounds of pharmaceutical significance.

3.4.5.1 Experimental Procedure

The main purpose of the TG analysis carried out here was to try to establish if the P(HEMA–co–VP) copolymers were, in fact, genuine random copolymers rather than mixtures of the two homopolymers. The particular instrument used was a Perkin–Elmer TGA 7 Thermogravimetric Analyzer, as shown in Fig. 3.21, while the dynamic TG operating conditions employed for each sample analysis were as shown in Table 3.12. In addition, the sample size was kept as uniform as possible in order to enable accurate comparisons to be made. The results are summarized in Fig. 3.22 and Table 3.13.

Fig. 3.21 : The Perkin–Elmer TGA 7 Thermogravimetric Analyzer.

Table 3.12 : Dynamic TG operating parameters and conditions used for polymer analysis.

TGA7 Method: PHEMACG1

Sample Information

Sample ID: P(HEMA) crosslinked
Operator ID: SARAYADEE

Parameters		Conditions	
Final Temp:	600.0 C	End Condition:	Start Temp
Start Temp:	50.0 C	Load Temp:	50.0 C
Scanning Rate:	20.0 C/min.	Go to Temp Rate:	200.0 C/min.
Y Range:	100.0 %	Event 1 Time:	0.00 min.
* Sample Weight:	4.470 mg.	Event 2 Time:	0.00 min.
		Delay Time:	0.00 min.

* variable according to sample

Perkin-Elmer TGA7

3.4.5.2 Comparison of Thermogravimetry (TG) Results

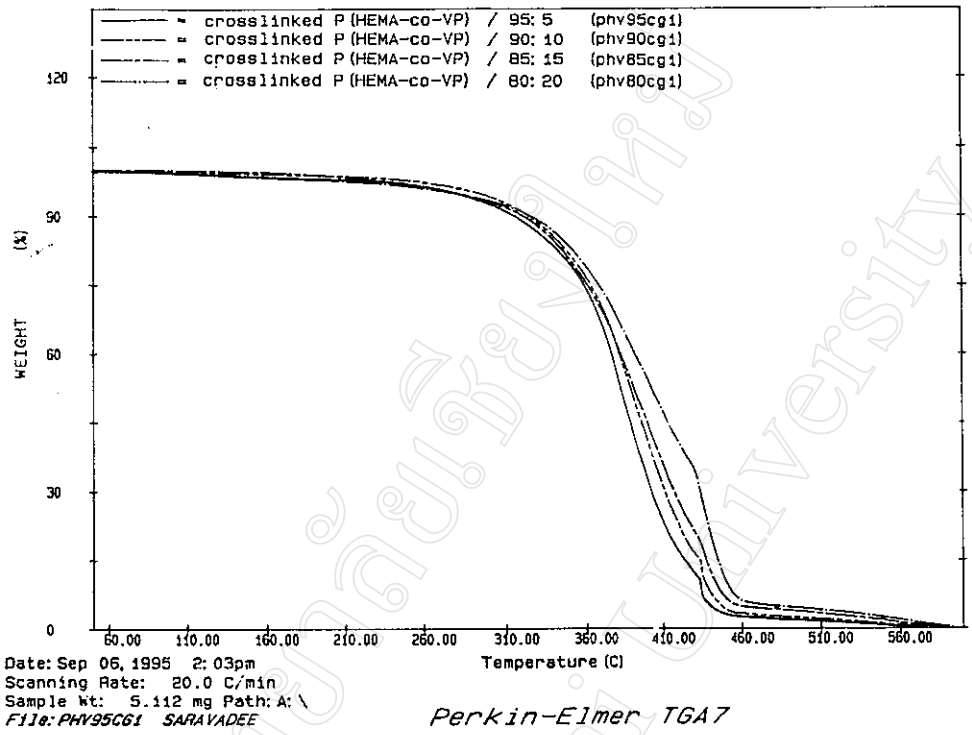

Fig. 3.22 : Dynamic TG thermograms of the P(HEMA–co–VP) copolymers.

Table 3.13 : Thermal degradation ranges of the P(HEMA) and PVP homopolymers and the P(HEMA–co–VP) copolymers.

Homopolymer or Copolymer	Composition* HEMA : VP (wt.%)	T_i** (°C)	T_f** (°C)	Residual weight percent (wt.%)
P(HEMA)	100 : 0	218	460	0.27
PVP	0 : 100	380	480	8.81
P(HEMA–co–VP)	92 : 8	235	464	1.03
P(HEMA–co–VP)	88 : 12	248	456	3.34
P(HEMA–co–VP)	84 : 16	247	461	4.83
P(HEMA–co–VP)	81 : 19	250	472	5.28

* from elemental analysis

** T_i = initial decomposition temperature

T_f = final decomposition temperature

3.5 Water Absorption Properties

3.5.1 Water Uptake – Time Profiles

The thin moulded sheets obtained directly from the 'in situ' bulk polymerization procedure previously described were of thickness 0.5 $\pm$ 0.1 mm, as measured with a micrometer. Rectangular pieces (2 cm $\times$ 4 cm) were cut and vacuum dried at 60°C to remove any absorbed moisture. The pieces were then immersed in distilled water at room temperature. The increasing water uptake of each sample was followed by measuring the increase in weight at various time intervals. It was found that, in general, the maximum water uptake was reached after about 2 hours. The increases in water uptake with immersion time for both homopolymers and copolymers are shown in Tables 3.14 and 3.15 and Figs. 3.23 and 3.24. The values were calculated from equation (3) below :

$$\textbf{Water Uptake} = \frac{\textbf{wt. of swollen polymer} - \textbf{wt. of dry polymer}}{\textbf{wt. of dry polymer}} \times \textbf{100 \%} \quad (3)$$

From Fig. 3.23, the water uptakes of the uncrosslinked and crosslinked P(HEMA) hydrogels attain constant values of about 58% and 50% by weight respectively after an immersion time of about 2 hours. This difference arises from the fact that the free volume between the polymer chains in the uncrosslinked P(HEMA) is more than in the crosslinked sample. Consequently, there is more space for water molecules to penetrate inside the polymer matrix. Also, the absence of crosslinks enables the matrix to swell (expand) more easily.

In Fig. 3.24, the range of P(HEMA–co–VP) copolymers are compared. The copolymers are essentially random copolymers. The results show that, as the amount of VP increases, the maximum water uptake also increases. This is presumably due to an increase in hydrophilicity. This is as would be expected since PVP is a water–soluble polymer.

Table 3.14 : The increasing water uptakes of P(HEMA) homopolymers immersed in distilled water for different times at room temperature (25°C).

Time (min)	Water Uptake (%)	
	uncrosslinked P(HEMA)	crosslinked P(HEMA)
5	16.4	14.2
10	21.6	17.0
15	25.5	20.1
20	27.8	22.0
25	31.7	24.2
30	34.2	28.0
35	36.8	27.6
40	42.4	29.2
45	41.7	32.1
50	45.0	39.0
55	48.2	*
60	48.1	39.7
65	50.5	*
70	*	41.8
80	53.8	43.1
90	56.4	*
100	56.5	48.2
110	56.3	48.1
120	57.0	49.6
150	58.4	*
180	57.5	*

* no data collected

Table 3.15 : The increasing water uptakes of crosslinked P(HEMA–co–VP) copolymers immersed in distilled water for different times at room temperature (25°C).

Time (min)	Water Uptake (%)			
	P(HEMA-co-VP) / 95 : 5	P(HEMA-co-VP) / 90 : 10	P(HEMA-co-VP) / 85 : 15	P(HEMA-co-VP) / 80 : 20
5	17.4	12.8	16.2	20.0
10	25.7	18.7	23.5	30.2
15	34.3	23.0	29.4	40.6
20	41.6	27.1	34.3	49.2
25	45.5	31.0	40.9	54.7
30	48.0	34.7	46.5	57.1
35	49.2	39.0	51.1	59.6
40	49.9	43.3	53.9	60.3
45	50.8	45.9	56.2	61.8
50	50.5	48.3	57.4	61.8
55	50.0	50.0	58.9	62.3
60	49.9	51.6	59.6	*
65	50.2	*	60.4	*
70	*	*	60.6	*
75	50.2	*	60.9	*
80	51.0	55.7	61.1	*
85	51.2	55.8	61.6	*
90	49.7	*	62.0	*

* no data collected

the weight ratios 95:5, 90:10, 85:15, 80:20 given at the heads of the columns refer to the comonomer feed compositions used in the copolymer syntheses

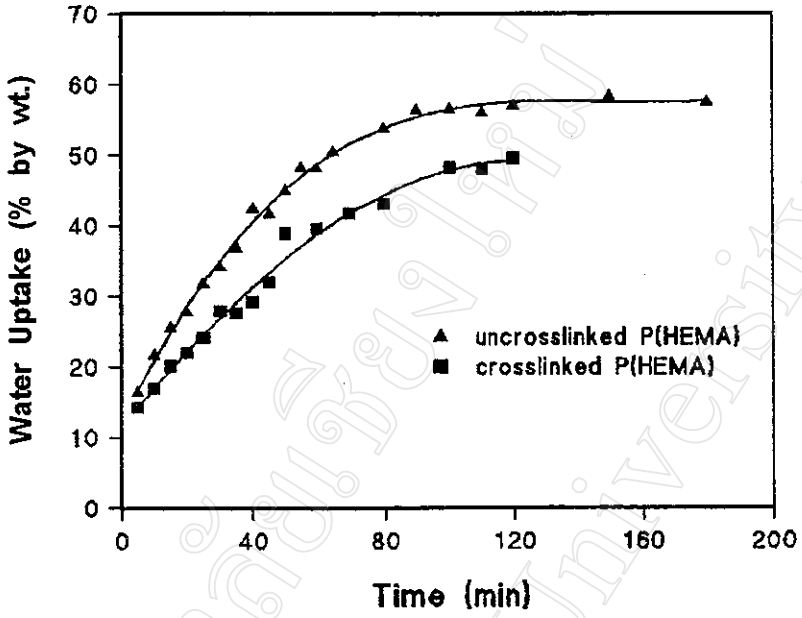

Fig. 3.23 : Effect of crosslinking on the water uptake of P(HEMA) at room temperature (25°C) ; (▲) uncrosslinked and (■) crosslinked with 1.0 % ethylene glycol dimethacrylate.

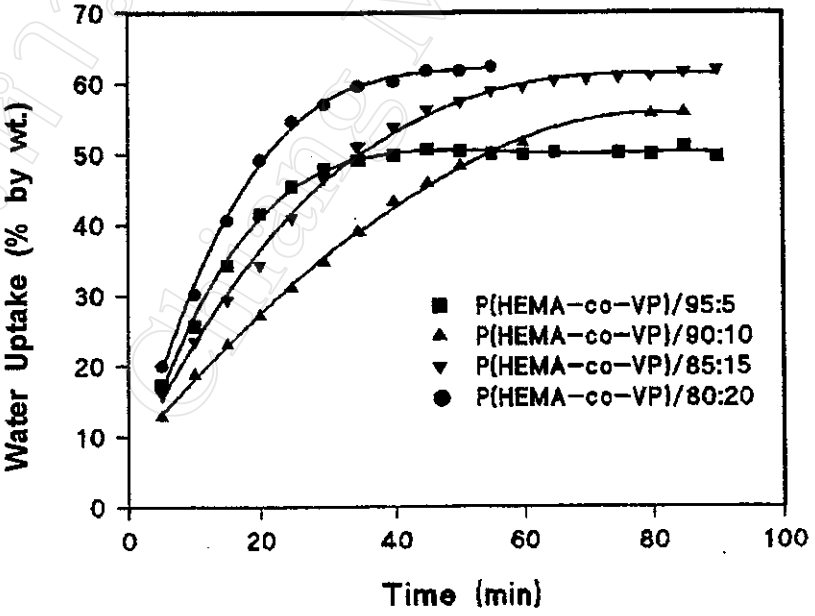

Fig. 3.24 : Effect of copolymer composition on the water uptake of crosslinked P(HEMA–co–VP) copolymers at room temperature (25°C).

Thus, the main conclusions that can be drawn from these results are :

(1) crosslinking decreases both the rate of water uptake and the final maximum value for P(HEMA)

(2) copolymerization of HEMA with a more hydrophilic monomer such as VP increases the water uptake of the hydrogel

A noticeable feature of Fig. 3.24 is that the curve for the P(HEMA–co–VP) / 95 : 5 copolymer is out of series with the other 3 curves and with the crosslinked P(HEMA) curve in Fig. 3.23. However, it seems unlikely that there would be anything special about this particular copolymer composition which would give rise to such a different response. Since there is no obvious explanation for this spurious result, it must be considered to be due to some peculiarity in sample condition. Apart from this one curve, the other curves show a consistent composition–dependent response.

3.5.2 Equilibrium Water Content [43, 44]

The ***equilibrium water content***, EWC, of a hydrogel is given conventionally by equation (4), as described previously in Chapter 1.

$$\text{EWC} = \frac{\text{wt. of swollen polymer} - \text{wt. of dry polymer}}{\text{wt. of swollen polymer}} \times 100\% \qquad (4)$$

The EWC of each sample was measured as follows. A thin rectangular test piece, 2 cm × 4 cm × 0.5 mm, was immersed in distilled water at room temperature until its water content became constant. It was then removed and any surface water carefully wiped off with a filter paper (Whatman No. 1). The sample was transferred to a pre–weighed sample bottle and accurately weighed. It was then dried to constant weight in a vacuum oven at 60°C. The EWC, as calculated from equation (4), was taken as the average value of at least three determinations. It should be

noted here that, because the EWC is calculated relative to the swollen weight (from equation 4 above), it is necessary less than the corresponding value of the maximum water uptake, referred to in the previous section, which is calculated relative to the dry weight (from equation 3 on page 56).

The EWC values of the P(HEMA) homopolymers and P(HEMA–co–VP) copolymers are compared in Table 3.16.

Table 3.16 : Equilibrium water contents (EWC) of P(HEMA) homopolymers and P(HEMA–co–VP) copolymers after immersion in distilled water at room temperature (25°C).

Homopolymer or Copolymer	Comonomer Feed HEMA : VP (wt. %)	Crosslinked or Uncrosslinked	EWC (%)	Avg EWC (%)
P(HEMA)	100 : 0	uncrosslinked	38.4, 38.0	38.2
P(HEMA)	100 : 0	crosslinked	34.8, 34.7, 34.5	34.7
PVP	0 : 100	uncrosslinked	*	–
PVP	0 : 100	crosslinked	*	–
P(HEMA–co–VP)	95 : 5	crosslinked	35.8, 33.8, 37.3	35.6
P(HEMA–co–VP)	90 : 10	crosslinked	37.6, 36.5, 39.2	37.8
P(HEMA–co–VP)	85 : 15	crosslinked	39.0, 38.8, 40.5	39.4
P(HEMA–co–VP)	80 : 20	crosslinked	40.5, 39.3, 42.9	40.9

* could not be measured because both the crosslinked and uncrosslinked PVP dissolved in water.

3.6 Water Vapour Transmission [45–47]

3.6.1 General Introduction

In designing an ideal temporary skin substitute, it is important to know the demands requiring fulfillment and the appropriate techniques to evaluate them. One of the most important physical requirements is the ability to control water loss from the wound surface. This arises from the fact that one of the major problems in the treatment of burn wounds is the prevention of total wound surface dehydration. Water loss by evaporation is an important factor in the maintenance of body hemostasis. Thermal injury to the skin destroys the semi-permeable membrane associated with the lipoprotein layer in the stratum corneum. The damage caused allows excessive water to be lost through the injured skin.

After thermal injury, the evaporative water loss from the wound surface can be some twenty times greater than normal skin [48]. Insensible water loss can place unacceptable demands on body metabolism, especially if the area of injury is extensive. Wenger [49] calculated that 2.43 MJ of energy are lost upon the evaporation of one litre of water and hence substantial evaporative water loss is associated with an abundant heat loss. This factor indicates the importance of limiting the water loss and hence heat loss during treatment. Heat loss can be reduced by maintaining a warm treatment environment. Insensible water loss can be reduced by the application of a temporary wound covering or a permanent graft. The ability to transport water vapour, as reflected in its water vapour transmission rate (WVT), is therefore an important function of the dressing. Hence, determination of its WVT is a valuable preclinical assessment of the dressing's potential performance characteristics.

An *in vitro* testing procedure recommended by the American Society for the Testing of Materials [45] has been commonly used to evaluate the WVT of skin substitutes. Two separate techniques, the **'Water Cup'** method (Procedure B) and the **'Inverted Cup'** method (Procedure BW) have been employed. The test material in film or sheet form is mounted on an aluminium cup assembly (Fig. 3.25) containing water and placed in a chamber under controlled temperature and

humidity conditions. The WVT is then determined by weighing the cup assembly at different time intervals. When the assembly is in an upright position, it is referred to as the **'Water Cup'** method. Alternatively, when the cup is inverted, so that the water is in direct contact with the sample, it is called the **'Inverted Cup'** method. Measurements are usually performed in a chamber maintained at 35°C and relative humidity of 55–60 %. A temperature of 35°C mimics the average temperature of the wound surface [48].

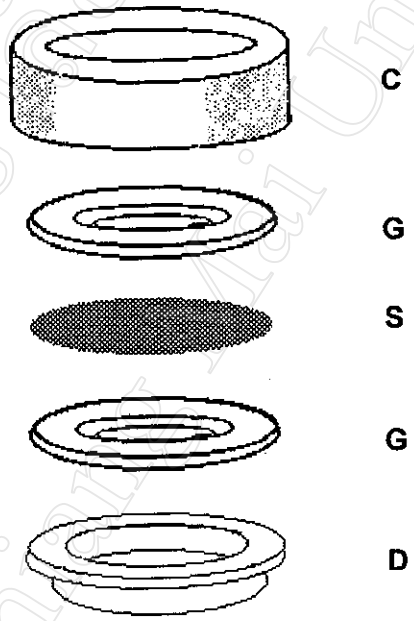

Fig. 3.25 : Expanded view of the aluminium cup assembly used for water vapour transmission (WVT) measurements.
C = cap, G = gaskets, S = test sample, D = cup

The main drawback associated with these methods is that a large difference in WVT is observed depending upon the geometry of the cup and the technique employed. This is attributed to the relative humidity gradient developed at the air–sample interface within the cup [46]. In the 'Water Cup' technique, the space between the sample and the water within the cup may not reach 100% relative humidity. Such an effect will reduce the observed WVT. Therefore, when using this *in vitro* technique, the 'Inverted Cup' method is usually preferred to the 'Water Cup' method as the boundary layer resistance is negligible and is less dependent on the geometry of the cup assembly. However, in this project, both methods were employed.

3.6.2 Test Procedure : 'Water Cup' Method [45]

Circular–shaped test specimens were cut from the hydrogel sheets using a template with an overall diameter of 7.0 cm. The mean thickness of each specimen was measured using a micrometer. When mounted in the cup assembly, the effective surface area of the specimen was 3.068×10^{-3} m^2. The test dish was then filled with distilled water to a level 3/4 ± 1/4 in (19 ± 6 mm) from the specimen. According to the test procedure, the water depth should be not less than 1/8 in (3 mm) to ensure coverage of the dish bottom throughout the test. The test specimen was attached to the dish by sealing in such a manner that the dish mouth defined the area of the specimen exposed to the vapour pressure in the dish. The dish assembly was then weighed and placed in a temperature–controlled incubator at 35.0 ± 1.0 °C, this being the zero–time (t = 0) for the experiment. The internal % humidity of the incubator was also recorded. The dish assembly was then re–weighed at various time intervals, each weighing giving a data point at a particular time. The rate of water vapour transmission, WVT, was calculated from equation (5) in which the slope of the plot of weight against elapsed time is divided by the exposed surface area of the specimen.

$$WVT = G / tA = (G / t) / A \quad (5)$$

where : G = weight change, g
t = time, hr
G / t = rate of weight change, g/hr
A = test area (cup mouth area), m^2
WVT = rate of water vapour transmission, g/hr m^2

The test results of the two homopolymers studied are given in the following Tables 3.18 – 3.21 and plotted as graphs of water loss against time in Figs. 3.26 – 3.28. As expected, the graphs are linear since the surface area from which the water evaporated was constant throughout the test.

Table 3.17 : Evaporative weight loss of water with time with no sample present, i.e., from the open cup.

Time (hr)	Temperature (°C)	Humidity (%)	Water Loss (g)
1	34.8	56	0.40
2	34.8	55	0.83
3	34.8	55	1.29
4	34.6	55	1.75
5	34.6	55	2.20
13	34.6	57	5.53
14	34.8	57	5.88
15	35.2	57	6.33
16	34.8	56	6.78
18	35.4	56	7.72
19	35.2	57	8.18
20	35.0	57	8.75
21	35.2	57	9.13
22	35.4	56	9.60
23	35.0	57	10.02
24	35.0	57	10.46

Table 3.18 : Water vapour transmission test results for uncrosslinked P(HEMA) : 'Water Cup' method.

Time (hr)	Temperature ($^{\circ}$C)	Humidity (%)	Water Loss (g)
1	35.0	50	0.01
2	35.0	49	0.01
4	35.0	49	0.01
7.75	34.6	47	0.12
10	35.6	48	0.19
11	34.6	50	0.23
12	35.0	50	0.27
13	35.0	48	0.30
15	34.8	48	0.39
23	34.4	51	0.67
25	35.2	51	0.75
26.5	35.2	48	0.84
28.5	34.8	48	0.87
29	35.2	49	0.89
30	35.4	48	0.99
32.5	35.0	47	1.05
34	35.0	47	1.09
36	35.4	50	1.19
38	34.8	50	1.25
50	34.8	50	1.73

Table 3.19 : Water vapour transmission test results for crosslinked P(HEMA) : 'Water Cup' method.

Time (hr)	Temperature ($^{\circ}$C)	Humidity (%)	Water Loss (g)
1	34.8	45	0.01
3	34.0	40	0.01
4	35.0	44	0.01
5	35.6	44	0.02
6	34.8	44	0.06
7	35.2	44	0.08
8	34.6	45	0.17
10.5	35.2	46	0.24
12	35.2	48	0.31
13	35.4	50	0.35
21.5	34.4	50	0.75
23	34.6	48	0.79
25	35.2	47	0.88
27	35.0	46	0.97
28	35.4	46	1.01
30	34.4	46	1.11
33	34.0	46	1.24
36	35.0	49	1.39
47	35.0	53	1.88
48	35.2	50	1.95
53	35.4	50	2.16

Table 3.20 : Water vapour transmission test results for uncrosslinked PVP : 'Water Cup' method.

Time (hr)	Temperature (°C)	Humidity (%)	Water Loss (g)
1	35.2	48	–
2	35.4	48	0.02
3	35.2	50	0.10
4	34.2	53	0.18
5	35.6	53	0.27
6	35.0	54	0.38
7	35.2	54	0.52
10	34.6	53	0.94
13	34.2	53	1.35
23	34.4	55	2.67
24	35.0	50	2.83
26	34.8	48	3.11
29	34.0	48	3.51
32	35.2	50	3.93
34	35.0	48	4.21
37	34.6	49	4.56
45	34.8	52	5.57
48	34.4	49	6.01
50	34.6	48	6.27
53	34.8	48	6.64

Table 3.21 : Water vapour transmission test results for crosslinked PVP : 'Water Cup' method.

Time (hr)	Temperature (°C)	Humidity (%)	Water Loss (g)
1	34.8	46	–
2	35.4	46	–
3	35.0	46	0.03
5	35.0	47	0.25
6.5	35.6	50	0.43
9	34.0	50	0.79
18	34.8	55	2.02
19	34.8	53	2.17
20	35.0	52	2.29
22.5	34.4	52	2.66
24	34.8	51	2.89
25	35.2	52	3.02
28.5	34.6	51	3.51
30	35.0	48	3.72
32	34.2	48	4.01
41.5	35.8	54	5.30
43	35.2	50	5.52
45	35.4	50	5.77
47	35.4	50	6.06
48	34.6	48	6.16
50	35.6	47	6.46
53.5	35.0	48	6.93

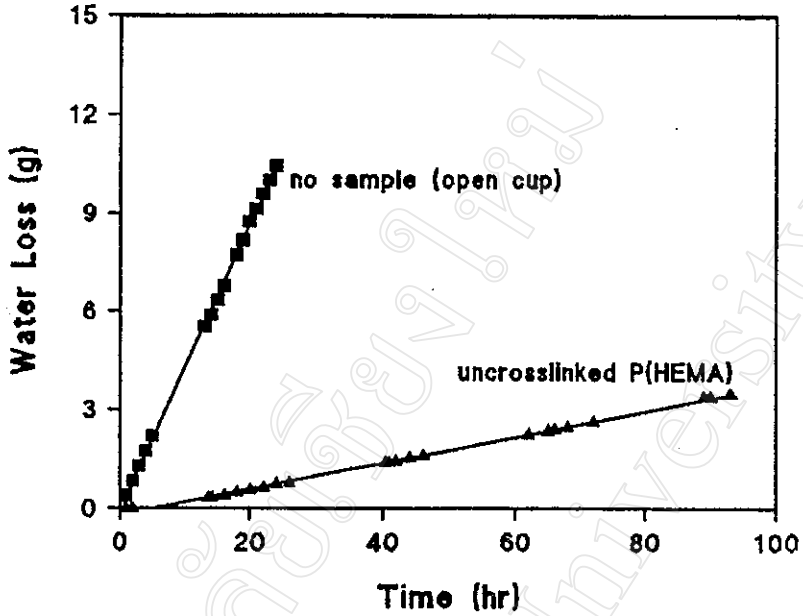

Fig. 3.26 : Plots showing the WVT rate for uncrosslinked P(HEMA) compared with the evaporative weight loss rate from the open cup : 'Water Cup' method.

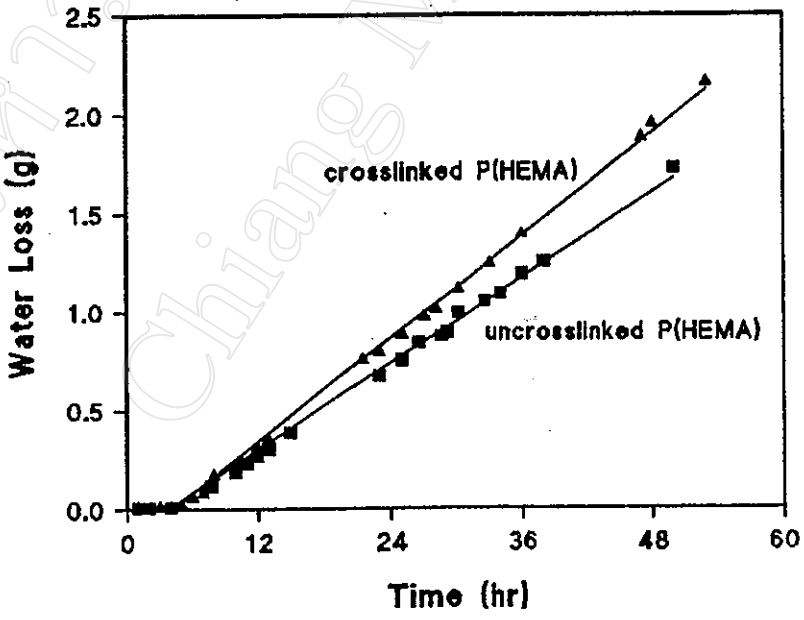

Fig. 3.27 : Comparison of the WVT rates for uncrosslinked and crosslinked P(HEMA) : 'Water Cup' method.

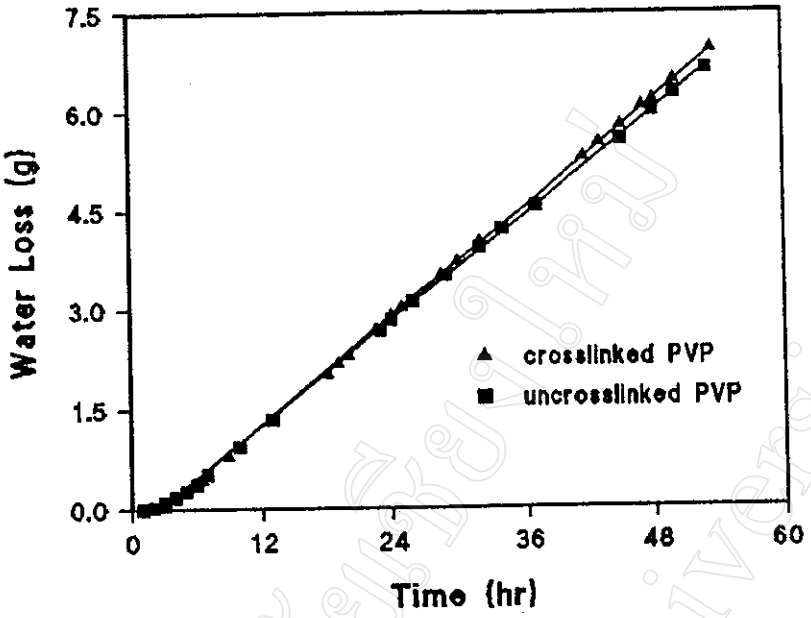

Fig. 3.28 : Comparison of the WVT rates for uncrosslinked and crosslinked PVP : 'Water Cup' method.

Table 3.22 : Comparison of the WVT rates for the P(HEMA) and PVP homopolymers studied in this work : 'Water Cup' method.

Sample [a]	Slope [b] (g/hr)	WVT (g/hr m^2)
No sample	0.435	141.8 [c]
P(HEMA) uncrosslinked	0.036	11.8
P(HEMA) crosslinked	0.043	14.2
PVP uncrosslinked	0.132	42.9
PVP crosslinked	0.136	44.4

WVT = water vapour transmission rate (from equation 5 on page 65)

a average sample thickness = 0.5 ± 0.1 mm

b slopes of the graphs in Figs. 3.25 – 3.27

c water vapour evaporation rate from the open cup

3.6.3 Test Procedure : 'Inverted Cup' Method [46, 50]

The test specimens used in the 'Inverted Cup' method were prepared in the same way as those used in the previous 'Water Cup' method, i.e. as circular thin sheets of diameter 7.0 cm. They were then immersed in distilled water to hydrate for at least 1 day, equilibrium water contents being reached in 4 to 5 hours. Since the resultant swelling caused the specimens to increase in diameter from 7.0 cm to 8.0 cm, they needed to be re–cut to size to fit the cup. Any surface water was removed with filter paper before the hydrated samples were fitted into the water vapour transmission assembly. The test dish was then filled with distilled water to a level 3/4 ± 1/4 in (19 ± 6 mm) from the specimen. This amount ensured that distension of the specimen due to the mass of water was not excessive nor that the reservoir would dry out during the test period. After testing for leakage of the assembled cup, the dish assembly was weighed, a suspending ring attached to the base, and the inverted cup suspended upside down inside the incubator, as shown below in Fig. 3.29. The dish assembly was weighed periodically in order to determine the WVT rate. The results are presented in the following Tables 3.23 – 3.28 and Figs. 3.30 – 3.32.

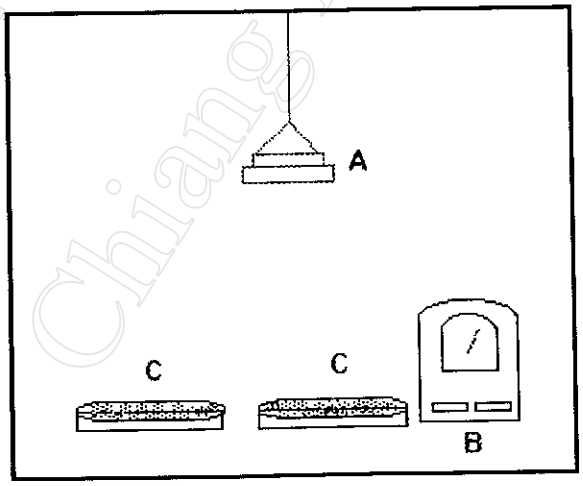

Fig. 3.29 : Internal arrangement employed inside the incubator for the 'Inverted Cup' method.
A = inverted cup, B = humidity meter, C = silica gel

Table 3.23 : Water vapour transmission test results for uncrosslinked P(HEMA) : 'Inverted Cup' method.

Time (hr)	Temperature (°C)	Humidity (%)	Water Loss (g)
1	35.0	53	0.37
2	34.2	54	0.62
3	35.4	54	0.93
4	34.6	55	1.14
5	35.6	56	1.41
6	35.6	50	1.67
7	34.6	51	1.92
10	34.4	50	2.65
11	35.0	53	2.92
13	35.6	53	3.37
14	34.2	55	3.63
23	34.8	55	5.71
26	35.4	55	6.43

Table 3.24 : Water vapour transmission test results for crosslinked P(HEMA) : 'Inverted Cup' method.

Time (hr)	Temperature (°C)	Humidity (%)	Water Loss (g)
1	34.6	52	0.39
2	35.2	52	0.64
3.5	34.2	52	1.03
4	35.4	56	1.16
5	35.0	52	1.43
6	34.6	53	1.66
7	35.2	54	1.93
8	34.4	55	2.18
10	34.0	55	2.64
12	34.6	50	3.15
15	34.4	51	3.88
23	35.8	56	5.77
26	35.0	52	6.51

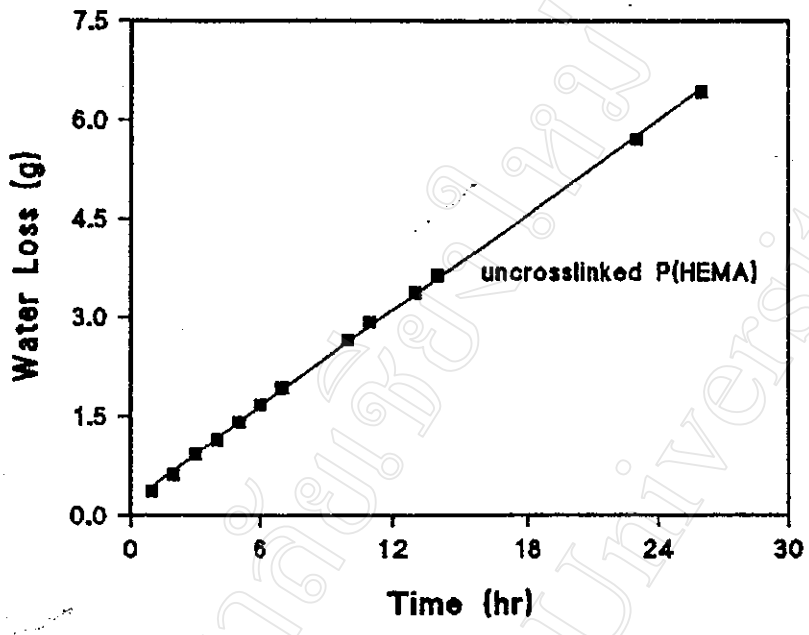

Fig. 3.30 : WVT plot for uncrosslinked P(HEMA) : 'Inverted Cup' method.

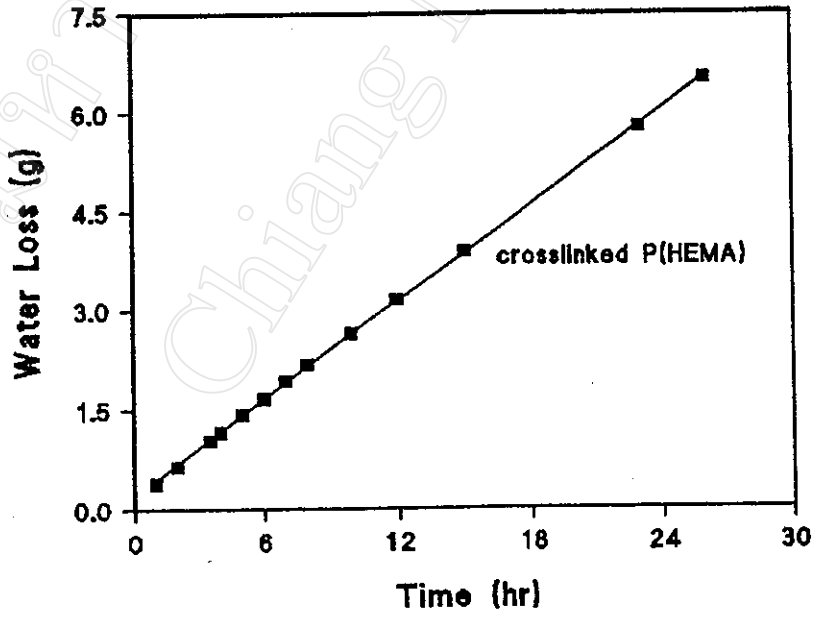

Fig. 3.31 : WVT plot for crosslinked P(HEMA) : 'Inverted Cup' method.

Table 3.25 : Water vapour tranmission test results for P(HEMA–co–VP) / 95 : 5 : 'Inverted Cup' method.

Time (hr)	Temperature (°C)	Humidity (%)	Water Loss (g)
1	34.8	55	0.35
2	35.4	55	0.65
3	34.6	55	0.98
6	35.4	55	1.80
7	35.6	52	2.12
9	34.4	54	2.71
10	35.2	55	3.00
11	34.8	55	3.31
19.5	35.0	60	5.63
21	34.6	56	6.07
22	35.2	55	6.44
24	34.8	56	6.95
26	34.8	58	7.54

Table 3.26 : Water vapour transmission test results for P(HEMA–co–VP) / 90 : 10 : 'Inverted Cup' method.

Time (hr)	Temperature (°C)	Humidity (%)	Water loss (g)
1	35.8	55	0.43
2	34.6	55	0.66
3	35.0	56	0.94
5	34.8	58	1.44
7	35.0	60	1.95
8.5	34.2	60	2.32
18	35.4	60	4.65
19	34.6	56	4.89
20	34.4	57	5.14
21	34.8	59	5.37
22	34.8	59	5.64
24	35.0	60	6.09
25	34.4	60	6.32

Table 3.27 : Water vapour transmission test results for P(HEMA–co–VP) / 85 : 15 : 'Inverted Cup' method.

Time (hr)	Temperature (°C)	Humidity (%)	Water Loss (g)
1	35.6	57	0.45
3	35.6	57	1.02
5	34.6	55	1.54
6	34.6	58	1.84
7	35.2	60	2.11
9	34.8	57	2.66
11	35.4	58	3.18
12	35.4	58	3.48
13	35.2	58	3.73
21.5	34.4	60	5.90
23	35.2	57	6.33
24	34.8	58	6.60
26	34.6	60	7.11

Table 3.28 : Water vapour transmission test results for P(HEMA–co–VP) / 80 : 20 : 'Inverted Cup' method.

Time (hr)	Temperature (°C)	Humidity (%)	Water Loss (g)
1	34.8	59	0.42
2	34.6	60	0.76
3	34.8	61	1.10
4	34.6	61	1.39
5	35.4	63	1.74
15	34.0	60	4.88
16	34.6	60	5.20
19	35.8	62	6.21
21	35.2	62	6.84
22	35.0	59	7.21
24	34.2	60	7.80
25	35.0	58	8.16
26	35.0	59	8.49

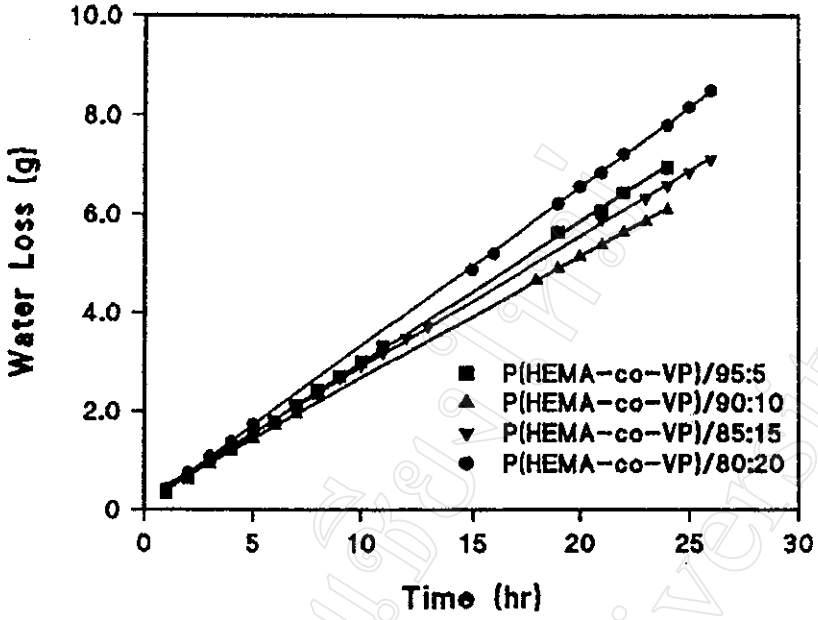

Fig. 3.32 : Comparison of the WVT rates for crosslinked P(HEMA–co–VP) copolymers : 'Inverted Cup' method.

Table 3.29 : Comparison of the WVT rates for the P(HEMA) homopolymers and P(HEMA–co–VP) copolymers studied in this work : 'Inverted Cup' method.

Sample [a]	Slope [b] (g/hr)	WVT (g/hr m^2)
P(HEMA) uncrosslinked	0.242	78.7
P(HEMA) crosslinked	0.244	79.5
P(HEMA-co-VP) / 95:5	0.286	93.2
P(HEMA-co-VP) / 90:10	0.246	80.3
P(HEMA-co-VP) / 85:15	0.265	86.3
P(HEMA-co-VP) / 80:20	0.321	104.7

WVT = water vapour transmission rate (from equation 5 on page 65)

[a] average sample thickness = 0.5 ± 0.1 mm

[b] slopes of the graphs in Figs. 3.29 – 3.31

From Table 3.29, it is again evident (as noted previously on page 60) that the P(HEMA–co–VP) / 95 : 5 copolymer response is inconsistent with the other 4 samples with which it forms a series. As in the previous case of its water uptake (Fig. 3.24 on page 59), its WVT rate is higher than it should be. This spurious result is difficult to explain in the light of the remaining data which is otherwise quite convincing in its indication that the WVT rate increases with increasing VP content in the copolymer.

3.6.4 Reproducibility of Results

In order to test the reproducibility of the water vapour transmission (WVT) results, repeat determinations were carried out for both the 'Water Cup' and 'Inverted Cup' methods. The samples and test conditions were similar to those previously described.

3.6.4.1 'Water Cup' Method

Table 3.30 : Water vapour transmission test results for uncrosslinked P(HEMA) : repeat determination.

Time (hr)	Temperature (°C)	Humidity (%)	Water Loss (g)
1	35.4	55	–
3	35.0	52	–
4	34.8	54	0.01
5	34.8	55	0.02
6	34.4	55	0.04
7	36.8	50	0.09
9	34.4	50	0.15
10	35.0	55	0.19
11	35.4	55	0.23
13.5	35.0	56	0.34
21.5	34.6	57	0.64
23	34.8	54	0.75
24	35.0	55	0.78
26.5	35.0	54	0.84

Table 3.31 : Water vapour transmission test results for crosslinked P(HEMA) : repeat determination.

Time (hr)	Temperature (°C)	Humidity (%)	Water Loss (g)
1	36.2	51	–
2	35.2	51	–
3	34.2	53	0.01
5.5	34.8	59	0.10
7	35.0	55	0.19
10	34.0	57	0.32
20	34.4	59	0.81
21	35.8	53	0.85
24	34.6	54	0.99
26	34.6	54	1.09
28	34.8	58	1.20

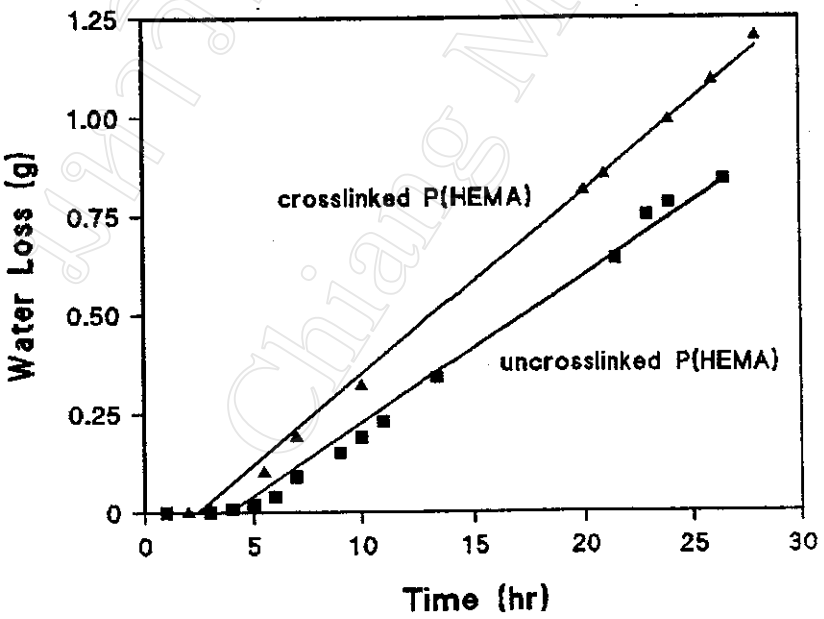

Fig. 3.33 : Comparison of the WVT rates for uncrosslinked and crosslinked P(HEMA) from the 'Water Cup' method : repeat determinations.

Table 3.32 : Water vapour transmission test results for uncrosslinked PVP : repeat determination.

Time (hr)	Temperature (°C)	Humidity (%)	Water Loss (g)
1	34.6	60	–
3	35.0	58	–
5	35.0	60	0.11
6	35.6	57	0.28
7	35.6	60	0.35
19	34.0	60	1.63
20	34.8	55	1.81
22	34.4	56	2.05
23	35.0	57	2.18
25	35.0	58	2.41
26	35.0	58	2.52
27	37.0	58	2.72

Table 3.33 : Water vapour transmission test results for crosslinked PVP : repeat determination.

Time (hr)	Temperature (°C)	Humidity (%)	Water Loss (g)
1	35.0	60	–
2	34.4	60	–
3	35.0	61	–
4	35.2	58	0.05
5	35.0	59	0.12
7	35.2	60	0.31
8	34.6	59	0.43
21	34.0	63	1.96
26	34.5	63	2.55

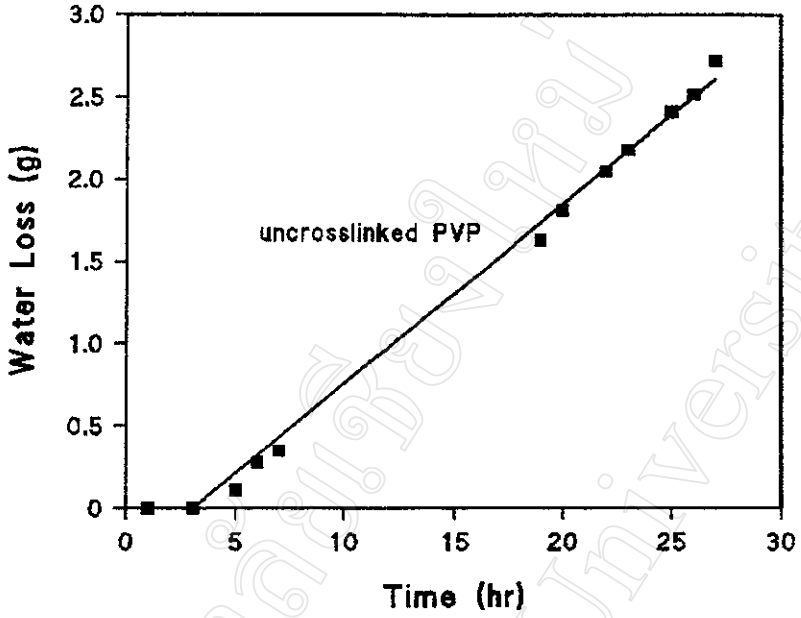

Fig 3.34 : WVT plot for uncrosslinked PVP from the 'Water Cup' method : repeat determination.

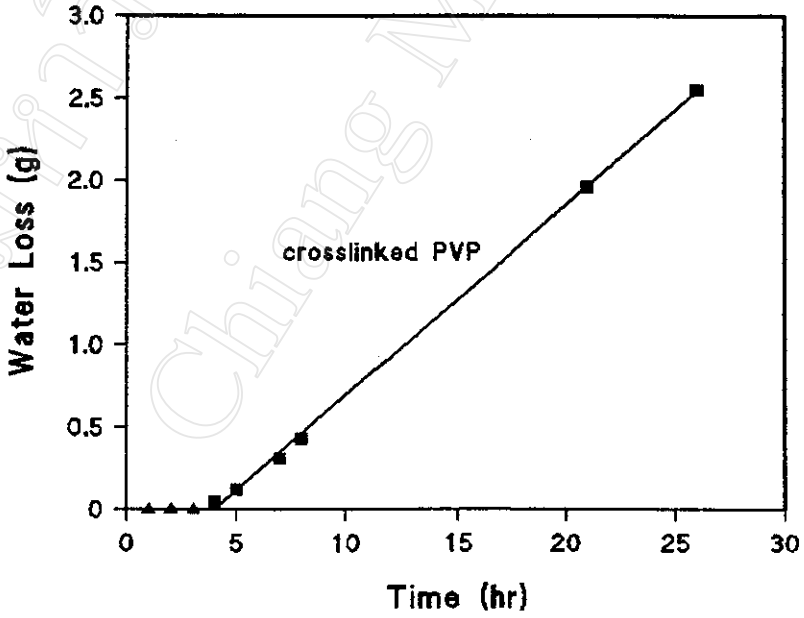

Fig 3.35 : WVT plot for crosslinked PVP from the 'Water Cup' method : repeat determination.

Table 3.34 : Reproducibility of WVT rates : 'Water Cup' method.

Sample	WVT (g/hr·m²)		Reproducibility [c]
	Previous [a]	Repeat [b]	(%)
uncrosslinked P(HEMA)	11.8	12.1	± 1.3
crosslinked P(HEMA)	14.2	15.0	± 2.7
uncrosslinked PVP	42.9	35.5	± 9.4
crosslinked PVP	44.4	37.6	± 8.3

[a] previous determinations : values taken from the previous Table 3.22 on page 71

[b] repeat determinations : values calculated from the slopes of the graphs in Figs. 3.33 – 3.35

[c] calculated as the % deviation from the average of the 2 determinations

3.6.4.2 'Inverted Cup' Method

Table 3.35 : Water vapour transmission test results for uncrosslinked P(HEMA) : repeat determination.

Time (hr)	Temperature (°C)	Humidity (%)	Water Loss (g)
1	35.2	57	0.44
3	37.0	60	1.00
5	34.2	59	1.56
6	35.0	60	1.84
18	35.6	60	4.85
19	34.8	59	5.14
20	34.4	60	5.39
22	34.6	60	5.96
23	34.6	58	6.21
24	34.6	58	6.47
25	34.4	59	6.76
26	34.8	60	6.97

Table 3.36 : Water vapour transmission test results for crosslinked P(HEMA) : repeat determination.

Time (hr)	Temperature (°C)	Humidity (%)	Water Loss (g)
1	34.2	59	0.36
2	34.6	59	0.58
3	34.6	59	0.88
4.5	34.6	59	1.18
8.5	35.6	60	2.16
19	36.2	60	4.73
20	34.8	58	4.96
21	34.0	60	5.22
24	35.0	60	5.91
26	35.4	60	6.42

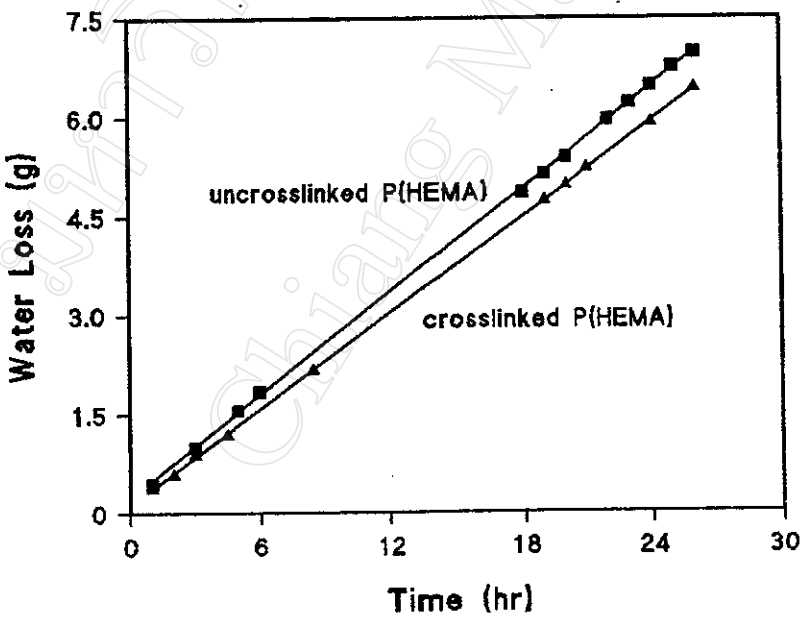

Fig. 3.36 : Comparison of the WVT rates for uncrosslinked and crosslinked P(HEMA) from the 'Inverted Cup' method : repeat determinations.

Table 3.37 : Reproducibility of WVT rates : 'Inverted Cup' method.

Sample	WVT ($g/hr \cdot m^2$)		Reproducibility [c]
	Previous [a]	Repeat [b]	(%)
uncrosslinked P(HEMA)	78.7	84.7	± 3.7
crosslinked P(HEMA)	79.5	79.0	± 0.3

[a] previous determinations : values taken from the previous Table 3.29 on page 77

[b] repeat determinations : values calculated from the slopes of the graphs in Fig. 3.36

[c] calculated as the % deviation from the average of the 2 determinations

3.6.4.3 General Conclusions on Reproducibility

From the reproducibility estimates (± %) given in Tables 3.34 and 3.37, the following general conclusions can be drawn :

1. In general, the WVT rates obtained from both the 'Water Cup' and 'Inverted Cup' methods are reproducible to within ± 10 % of the average value of the 2 determinations.
2. If only the P(HEMA) results are considered, then the reproducibility improves to within ± 4 %.
3. From the limited data available, there appears to be no significant difference in reproducibility between the 'Water Cup' and 'Inverted Cup' methods or any definite dependence upon crosslinking.

Taking into account all of the possible factors involved, the main reasons for the variation in WVT rates between samples of the same composition are considered to be due to control limitations in :

a. sample thickness (0.5 ± 0.1 mm)
b. incubator temperature (35.0 ± 2.0 °C)
c. % humidity inside the incubator (55 ± 10 %)
d. sample microstructure following post–curing (e.g., matrix porosity, crosslink density, molecular weight distribution, etc.)

3.7 Water Retention of Poly(hydroxyethyl methacrylate), P(HEMA), Hydrogels

The physical interaction between a hydrogel network and the water incorporated in it [51] leads to a gel–like structure containing firmly bound water. This ability to bind water is an important property of hydrogels in their use as wound covering materials. Lamke *et al* [48] showed that the average surface temperature of injured skin is 35°C and hence the water loss from hydrogels is usually measured in experiments carried out at this temperature. In this research project, only the P(HEMA) hydrogels were studied with respect to their water retention. The water retention was calculated according to equation (6).

The test specimens used in this determination were cut into a circular shape with a diameter of 7.0 cm and a thickness of about 0.5 mm. Each specimen was immersed in distilled water to hydrate to equilibrium for at least 1 day, as for the previous WVT 'Inverted Cup' experiments. The hydrated hydrogel specimen was then placed in an incubator at 35°C and the water loss by evaporation followed by measuring the decrease in weight at various time intervals. The results obtained are presented in Table 3.38 / Fig. 3.37 and Table 3.39 / Fig. 3.38 for the uncrosslinked and crosslinked P(HEMA) samples respectively.

In each case, the hydrogel lost about 35 % of its initial water content during the first 10 hours, after which its weight remained fairly constant. This ability to retain substantial amounts of water is of obvious significance in its application as a wound covering. At the same time, it is also important to recognize that the ability to lose water enables the hydrogel to take up exudate continuously from the wound surface.

$$\textbf{Water Retention} = \frac{\textbf{Water Content (at time t)}}{\textbf{Initial (Equilibrium) Water Content}} \times \textbf{100 \%} \qquad (6)$$

Table 3.38 : Water retention of uncrosslinked P(HEMA) hydrogel as a function of time.

Time (hr)	Temperature (°C)	Humidity (%)	Water Retention (%)
0	35.0	48	100.0
1	34.8	51	89.3
3.5	34.6	51	74.6
4	35.4	53	72.3
5	34.8	50	69.8
6.5	35.4	48	68.3
7	35.0	50	67.8
9	35.0	50	67.1
26	34.6	51	66.3

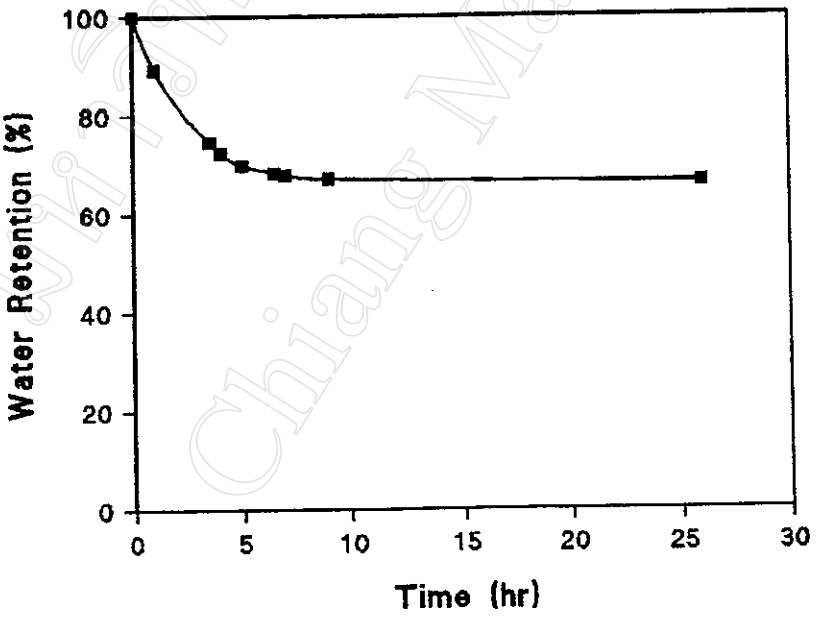

Fig. 3.37 : Time dependence of the water retention of the uncrosslinked P(HEMA) hydrogel.

Table 3.39 : Water retention of crosslinked P(HEMA) hydrogel as a function of time.

Time (hr)	Temperature (°C)	Humidity (%)	Water Retention (%)
0	35.2	49	100.0
1	34.8	53	88.9
2	36.2	45	78.4
3	35.2	45	73.8
4	35.0	45	71.0
5	34.8	45	69.4
11	34.0	42	68.5
19	34.6	47	68.2
25	34.8	45	67.6
29	35.0	45	67.6

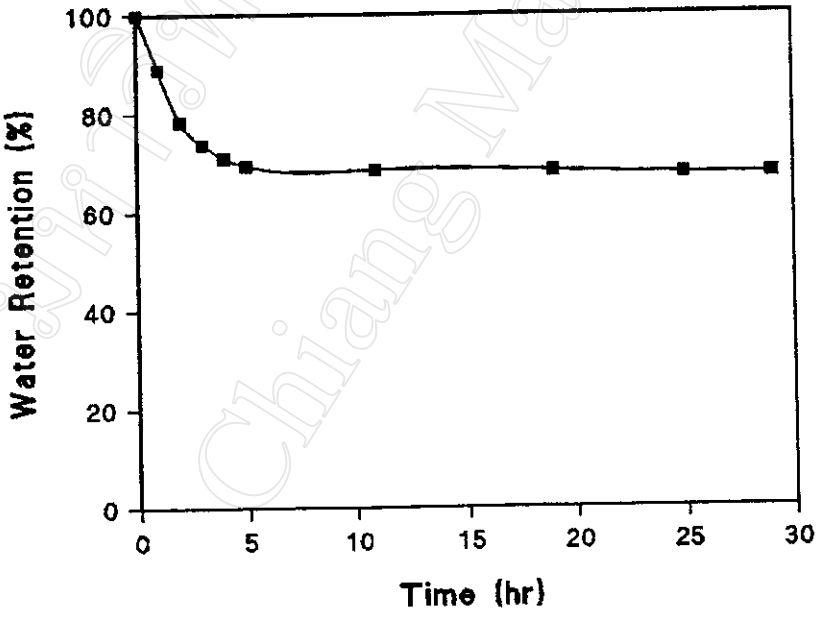

Fig. 3.38 : Time dependence of the water retention of the crosslinked P(HEMA) hydrogel.

3.8 Mechanical Property Testing

3.8.1 Stress – Strain Measurements [52]

In stress–strain measurements, the test specimen is subjected to a force that elongates it – causing, at the same time, the cross–sectional area to diminish – until the specimen breaks. For these stress–strain measurements, dumb–bell type test pieces are used which break between the predetermined guage marks, i.e., where the cross–sectional area is smallest. The shoulders of the test specimen serve to hold it in the grips of the testing machine. The grips are then driven apart with constant velocity by the drive mechanism of the machine. The load carried by the test specimen is automatically recorded as a function of the resulting elongation. The maximum load carried during a tension test is generally – but not always – identical with that at break.

When dividing the **load** (kg force) by the smallest **initial cross–sectional area**, A_o, of the test specimen, one obtains the corresponding **stress**, σ, which is, accordingly, the load per unit cross–sectional area. The **ultimate tensile strength** is then obtained by dividing the **maximum load**, L_{max}, carried by the initial cross–sectional area A_o.

$$\sigma = \frac{L_{max}}{A_o} \qquad (7)$$

Strain, ε, is the change per unit length in the linear dimension of the test specimen. This change is termed the **elongation**, Δl. The **ultimate strain**, ε, is therefore the elongation, $\Delta l_{max} = l_{max} - l_o$, that occurs at the maximum load, L_{max}, divided by the **initial length**, l_o.

$$\varepsilon = \frac{\Delta l_{max}}{l_o} \times 100\ \% \qquad (8)$$

From the data of ultimate tensile strength and the corresponding strain, one obtains a measure of the ultimate load that can be carried by the material. More informative for the characterization of a polymer, however, is a diagram of the entire

stress–strain experiment, i.e., a plot of stress, σ, versus strain, ε. Plastics may be subdivided into three classes according to their stress–strain diagrams (Fig. 3.39). In practice, there are gradual transitions between the three classes. The first class comprises compounds whose stress–strain curve is very steep and straight and flattens only slightly (curve I in Fig. 3.39). Similar to metals, these compounds are only slightly deformed even at relatively high loads. All thermosets, as well as some thermoplastics such as polystyrene and poly(methyl methacrylate), belong to this class, i.e., they are fairly inelastic and brittle.

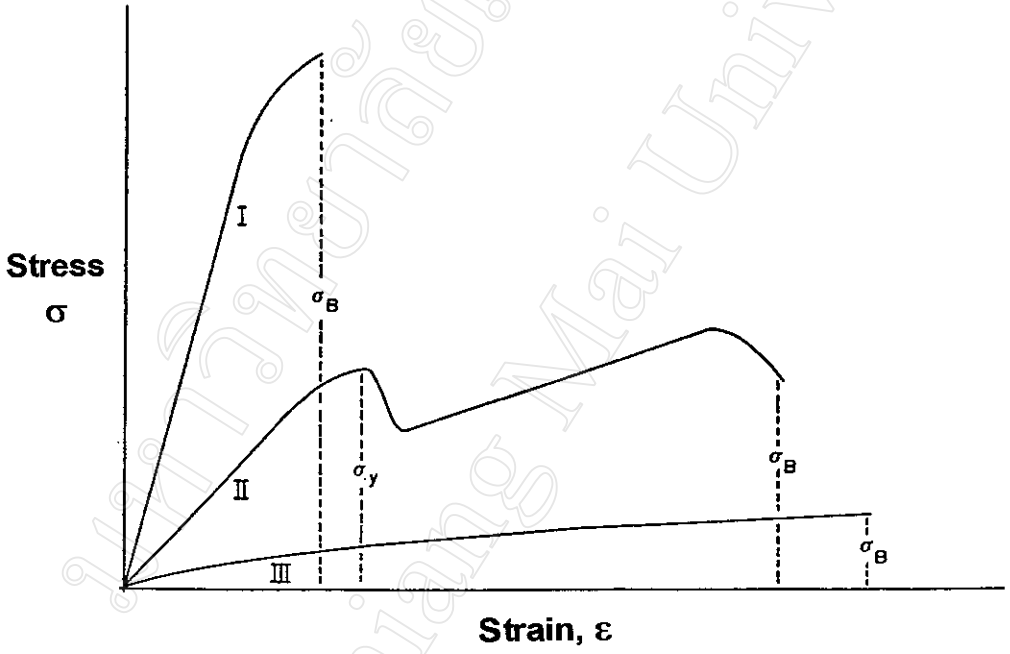

Fig. 3.39 : Stress–strain curves of polymeric materials [52].

σ_B = **stress at break point (ultimate strength)**

σ_y = **stress at yield point (yield strength)**

The second class exhibits the property of drawability which manifests itself in the stress–strain behavior shown in curve II, Fig. 3.39. Initially, these materials behave very much like those of curve I, i.e., the proportional limit is at very low strain values and deformation with increasing load is also only very small. Then, a very large extension occurs, although the load applied remains constant or even diminishes. The material begins to flow and the load–deformation curve continues nearly parallel to the abscissa. The point at which the material begins to flow is called the **yield point**. The stress at this point is denoted as the **yield strength**, σ_y, although the test specimen has not yet broken. During flow, the polymer molecules become extended and are oriented along the axis of the applied force. As soon as this process has come to completion, the stress again increases until the material breaks. The stress, σ, at this point is called the **ultimate strength**, σ_B, and the respective strain is denoted as **elongation at break**, ε_B. Many thermoplastics, such as the polyolefins, 6–nylon and 6–6 nylon, and unplasticized poly(vinyl chloride) (rigid PVC) belong to this class of polymers.

The third class comprises those polymers that are deformed considerably even at low loads. In the stress–strain diagram of these compounds, there is no sudden decrease in stress, i.e., there is no flow limit (curve III, Fig. 3.39). Furthermore, the mid–section of the curve is somewhat steeper than that of drawable compounds (curve II), i.e., the increase in strength resulting from reorientation of the macromolecules is a gradual one. If the force applied is increased further, failure results; the stress at this point is called the **ultimate strength**, σ_B, and the corresponding elongation, ε_B, is the **elongation at failure** (or elongation at break). This group comprises all plasticized thermoplastics (e.g., plasticized PVC), as well as rubbers (elastomers).

The **modulus of elasticity**, **E** (or **Young' s modulus**), which is a measure of the stiffness of the polymer, is obtained from the linear portion of the stress–strain curve. According to Hooke's Law, there is a linear relation between stress, σ, and strain, ε.

$$\sigma = E \varepsilon \qquad (9)$$

Consequently, Young's modulus corresponds to the slope of the linear portion of the stress–strain curve below the proportional limit :

$$E = \frac{\text{Stress}}{\text{Strain}} = \frac{\sigma}{\varepsilon} \qquad (10)$$

The Young's modulus is therefore defined as the load per unit area that is necessary to elongate, for example, a round rod by its own length. Materials with low modulus are elongated considerably even at low loads, while compounds with high modulus are deformed only slightly.

3.8.2 Testing Procedure and Results

In this work, the tensile properties of the hydrogels were determined using a Shimadzu Autograph AGS – 500A Universal Testing Machine (Fig. 3.40) employing a 5 kg load cell. The test specimens were immersed in distilled water to hydrate for at least 1 day before being cut into a dumb–bell shape with a Tensile Specimen Press. The thickness of each sample was then determined by a micrometer at four different points and the sample securely fixed in the jaws of the testing machine. The tests were carried out using a guage length of 40 mm. In total, five tests were run on each sample and the results averaged. The specimens were tested under the following conditions :

Load cell	:	5 kg
Load range	:	100
Cross–head speed	:	10 mm / min
Temperature	:	26.0 ± 1.0 °C
% Humidity	:	65 %
Chart ratio	:	5

Examples of the stress–strain curves for the crosslinked and uncrosslinked P(HEMA) hydrogels are shown in Figs. 3.41 and 3.42 respectively. The shapes of the curves are typical for all of the samples measured, including the P(HEMA-co-VP) copolymers. The results obtained from these stress–strain curves, and the calculated values of the various mechanical property terms, are summarized for each sample in Tables 3.40 – 3.45 and then collectively compared in Table 3.46.

Fig. 3.40 : The Shimadzu Autograph AGS – 500A Universal Testing Machine.

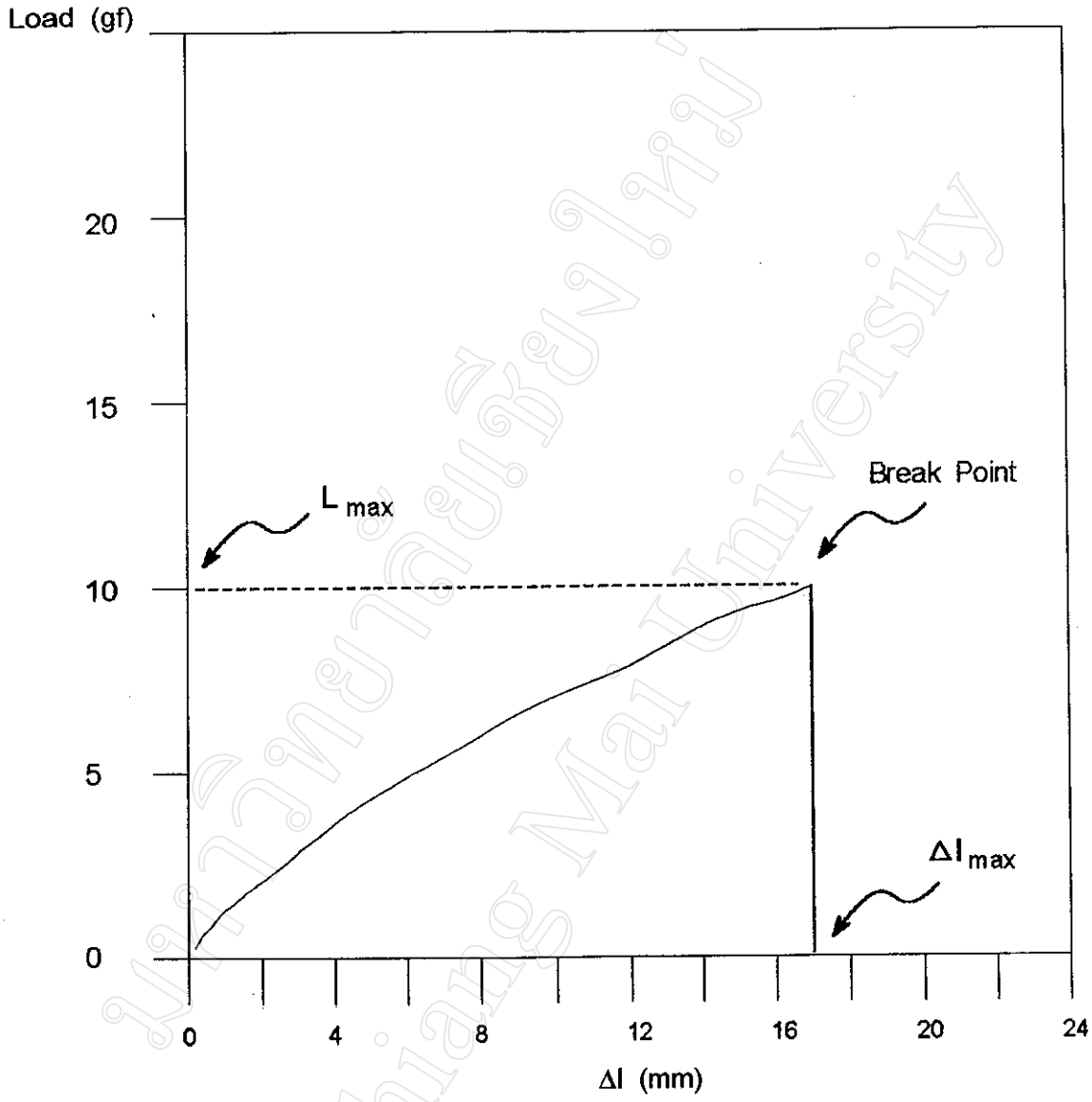

Fig. 3.41 : Stress – strain curve of the crosslinked P(HEMA) hydrogel, plotted as load against elongation. (Sample No. 1 in Table 3.40)

(Primary data as obtained directly from the testing machine.)

L_{max} = maximum load at break (gf = grams force)

Δl_{max} = elongation at break = $l_{max} - l_o$ (mm)

Table 3.40 : Mechanical property test results for the crosslinked P(HEMA) hydrogel.

Sample No.	Avg. Thickness (mm)	A_0 (mm^2)	Max. Load (L_{max}) (gf)	Max. Load (L_{max}) (N)	Stress (σ_B) ($N\ m^{-2}$ = Pa)
1	0.59	2.95	10.00	0.098	3.32×10^4
2	0.48	2.40	9.50	0.093	3.88×10^4
3	0.41	2.05	6.50	0.064	3.12×10^4
4	0.64	3.20	12.75	0.125	3.91×10^4
5	0.62	3.10	8.75	0.086	2.77×10^4

Sample No.	l_0 (mm)	Δl_{max} (mm)	Strain ε_B (%)
1	40.0	17.0	42.5
2	40.0	20.2	50.5
3	40.0	15.6	39.0
4	40.0	21.4	53.5
5	40.0	17.5	43.8

Sample No.	Tensile Strength ($gf\ mm^{-2}$)	Tensile Strength ($N\ m^{-2}$)	Elongation at Break (%)	Slope * ($gf\ mm^{-1}$)	Young's Modulus ($N\ m^{-2}$ = Pa)
1	3.39	3.32×10^4	42.5	0.588	7.82×10^4
2	3.96	3.88×10^4	50.5	0.470	7.68×10^4
3	3.17	3.12×10^4	39.0	0.417	7.98×10^4
4	3.98	3.91×10^4	53.5	0.596	7.31×10^4
5	2.82	2.77×10^4	43.8	0.500	6.33×10^4
Average	**3.46**	**3.40×10^4**	**45.9**	–	**7.42×10^4**

* slope (or average slope if non–linear) of the stress–strain curve = $L / \Delta l$

NOTE : details of the units used and calculations involved are given on the following page

Notes on Units :

gf = gram force (unit of load, i.e. force)

N = Newton = $kg\ m\ s^{-2}$ (S. I. Unit of force)

1 kgf = 9.81 N

Pa = Pascal (S. I. Unit of stress, strength, modulus)

Pa = $N\ m^{-2}$ = $kg\ m^{-1}\ s^{-2}$

Sample Calculations :

For Sample No. 1 in Table 3.40

Max. Load = L_{max} = 10.00 gf (from break point in stress-strain curve)

$$= \frac{10.00 \times 9.81}{10^3} \text{ N}$$

$$\mathbf{L_{max} = 0.098\ N}$$

Stress at Break = $\sigma_B = \frac{L_{max}}{A_o}$

$$\sigma_B = \frac{0.098}{2.95 \times 10^{-6}} \text{ N m}^{-2} \quad (= \text{Pa})$$

$$\mathbf{\sigma_B = 3.32 \times 10^4\ Pa}$$

Tensile Strength = Stress at Break = 3.32×10^4 Pa

Elongation at Break $= \frac{\Delta l_{max}}{l_o} \times 100\ \%$

$$= \frac{17.0 \times 100}{40.0} \%$$

$$\mathbf{\varepsilon_B = 42.5\ \%}$$

Young's Modulus = $E = \frac{\text{Stress}}{\text{Strain}} = \frac{L \times l_o}{A_o \times \Delta l}$

$$= \frac{(\text{slope of linear portion of stress-strain curve} \times l_o)}{A_o}$$

$$= \frac{(0.588 \times 40.0)\ \text{gf} \times 10^{-3} \times 9.81}{2.95 \times 10^{-6}} \text{ Pa}$$

$$\mathbf{E = 7.82 \times 10^4\ Pa}$$

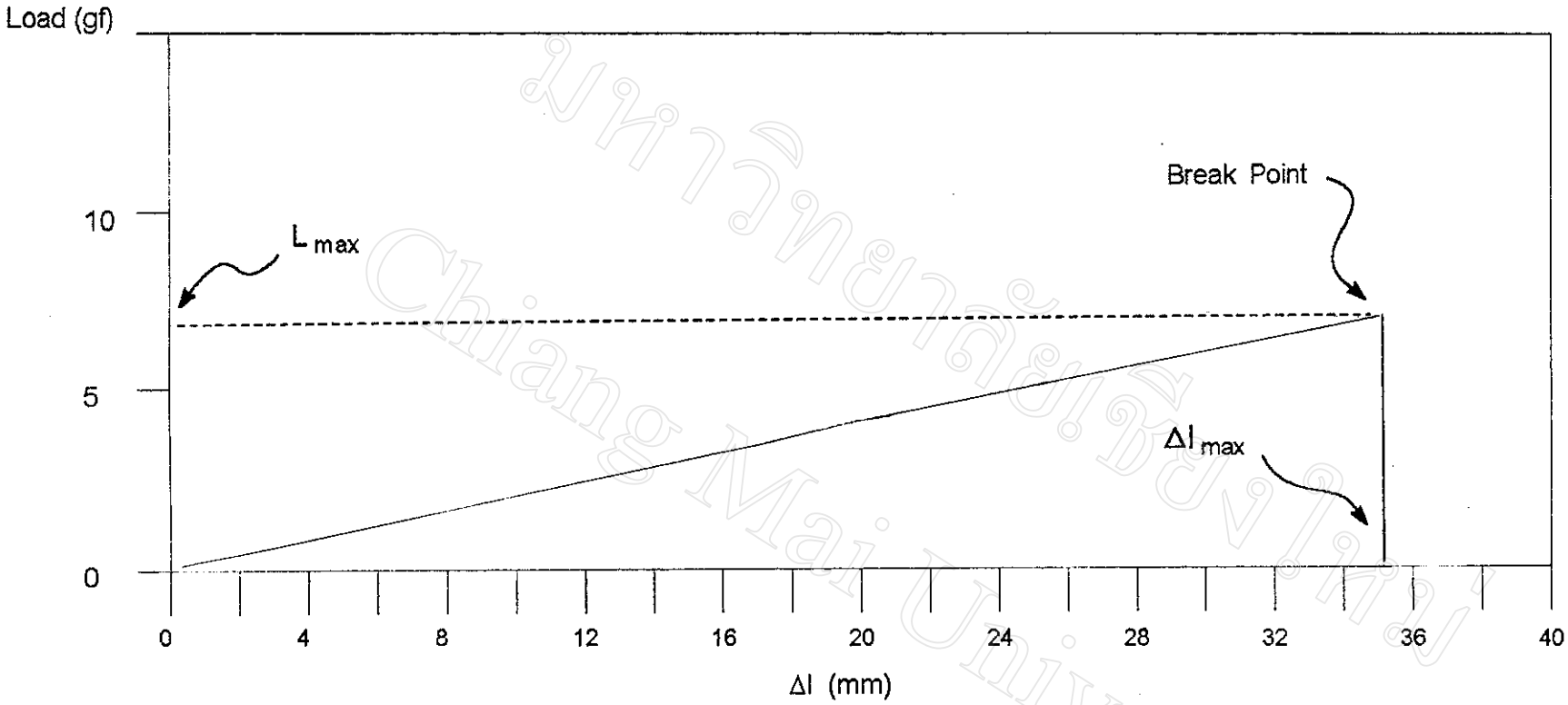

Fig. 3.42 : Stress – strain curve of the uncrosslinked P(HEMA) hydrogel, plotted as load against elongation. (Sample No. 1 in Table 3.41)

(Primary data as obtained directly from the testing machine.)

L_{max} = maximum load at break (gf = grams force)

Δl_{max} = elongation at break = $l_{max} - l_o$ (mm)

Table 3.41 : Mechanical property test results for the uncrosslinked P(HEMA) hydrogel.

Sample No.	Avg. Thickness (mm)	A_0 (mm^2)	Max. Load (L_{max}) (gf)	Max. Load (L_{max}) (N)	Stress (σ_B) ($N\ m^{-2}$ = Pa)
1	0.47	2.35	6.75	0.066	2.81×10^4
2	0.50	2.50	6.00	0.059	2.36×10^4
3	0.56	2.80	9.25	0.091	3.25×10^4
4	0.58	2.90	6.25	0.061	2.10×10^4
5	0.57	2.85	12.00	0.118	4.14×10^4

Sample No.	l_0 (mm)	Δl_{max} (mm)	Strain ε_B (%)
1	40.0	35.2	88.0
2	40.0	29.4	73.5
3	40.0	35.2	88.0
4	40.0	26.4	66.0
5	40.0	42.6	106.5

Sample No.	Tensile Strength ($gf\ mm^{-2}$)	Tensile Strength ($N\ m^{-2}$)	Elongation at Break (%)	Slope ($gf\ mm^{-1}$)	Young's Modulus ($N\ m^{-2}$ = Pa)
1	2.87	2.81×10^4	88.0	0.192	3.20×10^4
2	2.40	2.36×10^4	73.5	0.204	3.20×10^4
3	3.30	3.25×10^4	88.0	0.263	3.68×10^4
4	2.16	2.10×10^4	66.0	0.236	3.19×10^4
5	4.21	4.14×10^4	106.5	0.282	3.88×10^4
Average	**2.99**	**2.93×10^4**	**84.4**	–	**3.43×10^4**

NOTE : Calculations as on page 95

Table 3.42 : Mechanical property test results for the crosslinked P(HEMA–co–VP) / 95 : 5 hydrogel.

Sample No.	Avg. Thickness (mm)	A_0 (mm^2)	Max. Load (L_{max}) (gf)	Max. Load (L_{max}) (N)	Stress (σ_B) (N m^{-2} = Pa)
1	0.56	2.80	10.25	0.100	3.57×10^4
2	0.54	2.70	12.25	0.120	4.44×10^4
3	0.54	2.70	11.75	0.115	4.26×10^4
4	0.53	2.65	12.75	0.125	4.72×10^4
5	0.50	2.50	11.50	0.113	4.52×10^4

Sample No.	l_0 (mm)	Δl_{max} (mm)	Strain ε_B (%)
1	40.0	19.4	48.5
2	40.0	25.9	64.8
3	40.0	24.9	62.2
4	40.0	29.8	74.5
5	40.0	25.8	64.5

Sample No.	Tensile Strength (gf mm^{-2})	Tensile Strength (N m^{-2})	Elongation at Break (%)	Slope (gf mm^{-1})	Young's Modulus (N m^{-2} = Pa)
1	3.66	3.57×10^4	48.5	0.528	7.40×10^4
2	4.54	4.44×10^4	64.8	0.473	6.87×10^4
3	4.35	4.26×10^4	62.2	0.472	6.86×10^4
4	4.81	4.72×10^4	74.5	0.428	6.34×10^4
5	4.60	4.52×10^4	64.5	0.446	7.00×10^4
Average	**4.39**	**4.30×10^4**	**62.9**	–	**6.89×10^4**

NOTE : Calculations as on page 95

Table 3.43 : Mechanical property test results for the crosslinked P(HEMA–co–VP) / 90 : 10 hydrogel.

Sample No.	Avg. Thickness (mm)	A_0 (mm^2)	Max. Load (L_{max}) (gf)	Max. Load (L_{max}) (N)	Stress (σ_B) (N m^{-2} = Pa)
1	0.58	2.90	6.50	0.064	2.21×10^4
2	0.53	2.65	9.00	0.088	3.32×10^4
3	0.54	2.70	7.50	0.074	2.74×10^4
4	0.54	2.70	8.25	0.081	3.00×10^4
5	0.50	2.50	9.00	0.088	3.52×10^4

Sample No.	l_0 (mm)	Δl_{max} (mm)	Strain ε_B (%)
1	40.0	14.0	35.0
2	40.0	18.6	46.5
3	40.0	15.4	38.5
4	40.0	16.5	41.2
5	40.0	20.6	51.5

Sample No.	Tensile Strength (gf mm^{-2})	Tensile Strength (N m^{-2})	Elongation at Break (%)	Slope (gf mm^{-1})	Young's Modulus (N m^{-2} = Pa)
1	2.24	2.21×10^4	35.0	0.464	6.28×10^4
2	3.40	3.32×10^4	46.5	0.484	7.17×10^4
3	2.78	2.74×10^4	38.5	0.487	7.08×10^4
4	3.06	3.00×10^4	41.2	0.500	7.27×10^4
5	3.60	3.52×10^4	51.5	0.437	6.86×10^4
Average	**3.02**	**2.96×10^4**	**42.5**	–	**6.93×10^4**

NOTE : Calculations as on page 95

Table 3.44 : Mechanical property test results for the crosslinked P(HEMA–co–VP) / 85 : 15 hydrogel.

Sample No.	Avg. Thickness (mm)	A_0 (mm^2)	Max. Load (L_{max}) (gf)	Max. Load (L_{max}) (N)	Stress (σ_B) (N m^{-2} = Pa)
1	0.59	2.95	7.00	0.069	2.34×10^4
2	0.53	2.65	8.50	0.083	3.13×10^4
3	0.48	2.40	7.75	0.076	3.17×10^4
4	0.40	2.00	6.50	0.064	3.20×10^4
5	0.39	1.95	4.25	0.042	2.15×10^4

Sample No.	l_0 (mm)	Δl_{max} (mm)	Strain ε_B (%)
1	40.0	14.9	37.2
2	40.0	15.9	39.8
3	40.0	16.9	42.2
4	40.0	13.9	34.8
5	40.0	10.3	25.8

Sample No.	Tensile Strength (gf mm^{-2})	Tensile Strength (N m^{-2})	Elongation at Break (%)	Slope (gf mm^{-1})	Young's Modulus (N m^{-2} = Pa)
1	2.37	2.34×10^4	37.2	0.470	6.25×10^4
2	3.21	3.13×10^4	39.8	0.534	7.91×10^4
3	3.23	3.17×10^4	42.2	0.458	7.49×10^4
4	3.25	3.20×10^4	34.8	0.468	9.18×10^4
5	2.18	2.15×10^4	25.8	0.413	8.31×10^4
Average	**2.85**	**2.80×10^4**	**36.0**	–	**7.83×10^4**

NOTE : Calculations as on page 95

Table 3.45 : Mechanical property test results for the crosslinked P(HEMA–co–VP) / 80 : 20 hydrogel.

Sample No.	Avg. Thickness (mm)	A_0 (mm^2)	Max. Load (L_{max}) (gf)	(N)	Stress (σ_B) (N m^{-2} = Pa)
1	0.56	2.80	9.50	0.093	3.32×10^4
2	0.46	2.30	6.50	0.064	2.78×10^4
3	0.44	2.20	7.50	0.074	3.36×10^4
4	0.43	2.15	7.50	0.074	3.44×10^4
5	0.23	1.15	5.00	0.049	4.26×10^4

Sample No.	l_0 (mm)	Δl_{max} (mm)	Strain ε_B (%)
1	40.0	23.8	59.5
2	40.0	17.8	44.5
3	40.0	23.0	57.5
4	40.0	22.7	56.8
5	40.0	26.3	65.8

Sample No.	Tensile Strength (gf mm^{-2})	(N m^{-2})	Elongation at Break (%)	Slope (gf mm^{-1})	Young's Modulus (N m^{-2} = Pa)
1	3.39	3.32×10^4	59.5	0.399	5.59×10^4
2	2.83	2.78×10^4	44.5	0.365	6.23×10^4
3	3.41	3.36×10^4	57.5	0.326	5.81×10^4
4	3.49	3.44×10^4	56.8	0.330	6.02×10^4
5	4.35	4.26×10^4	65.8	0.190	6.48×10^4
Average	**3.49**	**3.43×10^4**	**56.8**	–	**6.03×10^4**

NOTE : Calculations as on page 95

The mechanical property values for the samples studied, as given in Tables 3.40 – 3.45, are brought together for ease of comparison in Table 3.46 below. These values determine how strong, flexible and pliable each material will be, properties which would be important to its application as a wound covering. The values given in Table 3.46 are the average values of the 5 determinations that were carried out for each sample.

Table 3.46 : Comparison of the (average) mechanical property values for the crosslinked and uncrosslinked P(HEMA) and crosslinked P(HEMA–co–VP) hydrogels.

Sample	Tensile Strength ($N\ m^{-2}$)	Elongation at Break (%)	Young's Modulus ($N\ m^{-2}$)
crosslinked P(HEMA)	3.40×10^4	45.9	7.42×10^4
uncrosslinked P(HEMA)	2.93×10^4	84.4	3.43×10^4
crosslinked P(HEMA–co–VP) / 95 : 5	4.30×10^4	62.9	6.89×10^4
crosslinked P(HEMA–co–VP) / 90 : 10	2.96×10^4	42.5	6.93×10^4
crosslinked P(HEMA–co–VP) / 85 : 15	2.80×10^4	36.0	7.83×10^4
crosslinked P(HEMA–co–VP) / 80 : 20	3.43×10^4	56.8	6.03×10^4

Thus, the main conclusions that can be drawn from these results are :

(1) On comparing the crosslinked and uncrosslinked P(HEMA) samples, the effects of crosslinking are (a) to increase the tensile strength and (b) to decrease the elongation at break, thus increasing the modulus. This is as would be expected since the purpose of crosslinking is to tie the polymer chains together, thereby increasing the energy required to make them deform. Of these two effects, the decrease in elongation seems to be the more pronounced.

(2) On comparing the crosslinked P(HEMA) and P(HEMA–co–VP) samples, the effect of increasing the VP content over the 0 – 20 % range is more difficult to define. The results are rather inconclusive with no definite trend. It would seem therefore that VP, as the modifying comonomer, influences the copolymer's hydrophilicity (water absorption / transmission) more than its mechanical properties.